Available online at www.sciencedirect.com

ScienceDirect

journal homepage: www.elsevier.com/locate/he

Review Article

Hydrogen production through photoreforming processes over Cu_2O/TiO_2 composite materials: A mini-review

Marica Muscetta [a], *Roberto Andreozzi* [a], *Laura Clarizia* [a,*], *Ilaria Di Somma* [b,**], *Raffaele Marotta* [a]

[a] *Dipartimento di Ingegneria Chimica, dei Materiali e della Produzione Industriale, Università di Napoli Federico II, p. le Tecchio 80, Napoli, 80125, Italy*

[b] *Istituto di Ricerche sulla Combustione, Centro Nazionale delle Ricerche IRC CNR, p.le Tecchio 80, Napoli, 80125, Italy*

HIGHLIGHTS

- First comprehensive literature survey on Cu_2O/TiO_2 photocatalysts for H_2 generation.
- Comparison of preparation methods, organics and pH used, and efficiencies recorded.
- Clear information on analytical techniques uniquely identifying Cu_2O in Cu_2O/TiO_2.
- Insight into reaction mechanisms for H2 evolution over Cu_2O/TiO_2 photocatalysts.

GRAPHICAL ABSTRACT

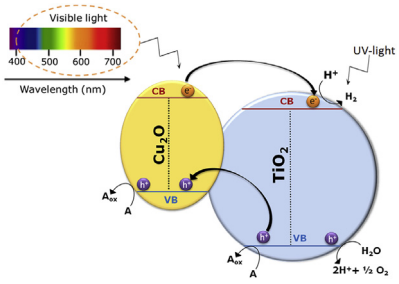

ARTICLE INFO

Article history:
Received 8 April 2020
Received in revised form
18 July 2020
Accepted 24 July 2020
Available online 17 August 2020

Keywords:
Cuprous oxide
Cu_2O/TiO_2 composite

ABSTRACT

Cu_2O is a promising low-cost semiconductor exhibiting a narrow band gap. The combination of p-type Cu_2O with n-type TiO_2 results in a p-n heterojunction highly beneficial to photocatalytic processes, due to the resulting capability of (i) absorbing visible light irradiation and (ii) promoting charge carrier separation.

An intense scientific activity has been recorded in the field of H_2 generation through water photosplitting and organic photoreforming over Cu_2O/TiO_2-based composites.

This literature survey aims at clarifying conflicting information on the preparation, characterization, and use of Cu_2O/TiO_2 composites for H_2 evolution. Detailed information on analytical techniques devoted to uniquely identifying Cu_2O has been provided. Preparation method, effect of pH, effect of sacrificial agent, chemical stability of Cu_2O/TiO_2

* *Corresponding author.*
** *Corresponding author.*
E-mail addresses: laura.clarizia2@unina.it (L. Clarizia), idisomma@unina.it (I. Di Somma).

https://doi.org/10.1016/j.ijhydene.2020.07.225

Photocatalytic hydrogen generation
Visible light active photocatalysts

composites, and reaction mechanisms have been critically discussed. The highest efficiency values obtained over Cu_2O/TiO_2 photocatalysts have been reported. A solid groundwork on which developing new effective and low-cost materials for H_2 generation has been provided.

Contents

Introduction

Concerns over environmental protection and fossil fuel depletion prompted the research in the past decade towards new and clean processes for energy production through renewable sources. Among them, photocatalytic water splitting is one of the most promising for production of both hydrogen and, indirectly, electricity through proton exchange fuel cells [1–7]. Since Fujishima and Honda's pioneering work on photocatalytic reduction of water on a single crystal of TiO_2, increasing research attention has been devoted to study and develop innovative photocatalytic systems for water photosplitting or organic photoreforming [8–18]. As part of these processes, titanium dioxide has been proposed as a photocatalyst due to its interesting properties, such as wide chemical stability, large availability, and environmental affinity. However, major drawbacks of using titanium dioxide for photocatalytic solar applications include narrow absorption range and low charge carrier mobility [19,20]. TiO_2 anatase or anatase/rutile mixed crystalline phases show significant electron-hole pair recombination during photocatalytic hydrogen evolution, thus fatally undermining the overall photoefficiency. Surface or structural defects may be introduced by loading noble or transition metal ions [19,21–23]: the low energy Fermi level of noble metals allows electron transfer from TiO_2 to the metal itself [24]. Such process results into a more efficient charge carrier separation, with enhanced efficiency for hydrogen generation [25]. Many studies indicated that loading TiO_2 surface with precious metal nanoparticles (gold, platinum, palladium, etc.) makes the resulting catalyst suitable for photocatalytic hydrogen production, although such species are expensive and, in some cases, rare [26]. During last decade, the identification of other

low-cost metals capable of exerting the same role of co-catalyst has been attempted in order to replace the use of noble metals. According to an extensive literature review, copper could be one of these elements [27–30]. Moreover, as TiO_2 is a wide band-gap semiconductor capable of absorbing only ultraviolet radiations, numerous visible light active combined photocatalysts have been prepared and investigated as a result of combining TiO_2 with other semiconductor species. Copper, in the form of zerovalent species or oxide, has been often proposed as TiO_2 co-catalyst able to remarkably enhance hydrogen production rate [31–37]. In previous papers by some of the Authors, an insight into copper modified-TiO_2 catalysts for hydrogen generation has been proposed with the aim of deeply understanding their electronic structure, surface properties, effect of sacrificial agent and solution pH, and further crucial synthesis and operating variables [38].

A great interest in the possibility of hydrogen generation through organic photoreforming by combining Cu_2O (i.e. p-type semiconductor) and TiO_2 (i.e. n-type semiconductor) has recently emerged. Preparation, reaction mechanism, photocatalytic and chemical stability are just some of the topics which have so far received the highest attention. On the other hand, poor information on the efficiency for hydrogen generation of such materials has been generally recorded. Literature findings on all these aspects was herein critically reviewed with the aim of clarifying some controversial indications found, with the purpose of helping achieve further advances in the development of efficient and cheap photocatalysts for hydrogen generation through solar organic photoreforming.

Cu_2O as semiconductor and p-n type heterojunction with titania

Cu_2O-based materials are employed for a wide range of applications, such as sensing, desulfurization, disinfection, organic synthesis, photodegradation, photovoltaics, and photocatalysis[13,39–51]. In particular, recent literature findings indicate a growing interest towards Cu_2O as cocatalyst on titanium dioxide for photocatalytic hydrogen evolution [52–54] with performances comparable with Ag and Au [55–57].

Cu_2O is a typical p-type semiconductor exhibiting a narrow band gap of 2.2 eV, whereas TiO_2 is an extensively investigated n-type semiconductor. Their combination may result in a p–n heterojunction, which can (i) absorb radiation within the solar spectrum [58–60] and (ii) increase photogenerated charge carrier separation, leading to higher photocatalytic efficiencies [61–63].

Within the crystalline structure of n-type TiO_2 and p-type Cu_2O the majority of charge carriers are negative electrons and positive holes, respectively. As soon as the p-n heterojunction is formed at the TiO_2/Cu_2O interface, the difference in Fermi levels drives the charge carrier flow until an equilibrium state in which the Fermi level is constant at any point in the system is reached, as schematically shown in Fig. 1 [64,65]. As a result of interfacial charge flow, an electric field from TiO_2 to Cu_2O and band bending are formed due to resulting local zones of Cu_2O and TiO_2 carrying excess negative and positive charges, respectively. Finally, the arising p-n heterojunction promotes the photocatalytic hydrogen generation process by enhancing electron flow from to Cu_2O to TiO_2.

Preparation of Cu_2O/TiO_2 composite materials

From literature indications, the preparation methods of Cu_2O/TiO_2 composite photocatalysts primarily differ in terms of TiO_2 type used. On the basis of this consideration, a first classification is herein made by considering the TiO_2 type. In particular, the papers analyzed in the present investigation can be classified in two different classes: a first class using TiO_2 in its commercial mixed phase (i.e. P25–TiO_2), and a second one employing home-prepared titanium dioxide. In the latter case, the different preparation method will be not discussed in the present work. As concerns Cu_2O, Cu(II) is the commercially available form of copper species with highest chemical stability, hence most of the Cu_2O/TiO_2 preparation procedures found in the literature survey involve the use of a cupric salt, such as cupric nitrate, perchlorate, or sulfate. Cupric species, generally dissolved in aqueous solution, are selectively reduced in the presence of titanium oxide, so that cuprous ion can be promptly incorporated on the surface or in the crystalline structure of TiO_2, using different reduction methods as well as reducing agents.

Several reduction methods are reported in the next paragraphs. Moreover, as reported in Table 1, others distinguishing factors found in the preparation of Cu_2O/TiO_2 photocatalysts are the deposition method of active species (e.g. impregnation/calcination, photodeposition, electrochemical deposition, etc.) and the employment of selected cocatalysts (e.g. WS_2, Au, Pt, etc.). Some examples of distinguishing factors in the preparation of Cu_2O–TiO_2 composite materials are briefly given hereunder.

Reducing agents

Glucose

Several authors employed glucose as reducing agents in the preparation procedure of Cu_2O/TiO_2 photocatalysts for hydrogen evolution [60,66–68]. Segovia-Guzman [66] et al. prepared Cu_2O/TiO_2 samples by impregnation followed by a microwave-assisted method employing glucose as reducing and stabilizing agent at two levels of concentration. To this aim, a fixed amount of P25–TiO_2 was added to deionized water at room temperature together with an aliquot of glucose, $CuCl_2$, and NaOH solutions. The suspension was then magnetically stirred at room temperature for and heated at 120 °C microwave system to obtain a hydrothermal effect. After centrifugation, the precipitates were washed and dried at 70 °C. The formation of cuprous oxide was clearly demonstrated by XRD and XPS spectra. After using such catalyst for H_2 generation through glycerol photoreforming under UV–visible irradiation through a metal halide lamp, the chemical stability of the recycled photocatalyst was confirmed by XPS results, which excluded the occurrence of Cu_2O transformation after the photocatalytic process.

Tamiolakis et al. [67] prepared Cu-loaded mesoporous TiO_2 nanoparticles (MTA) with different Cu_2O content by chemical

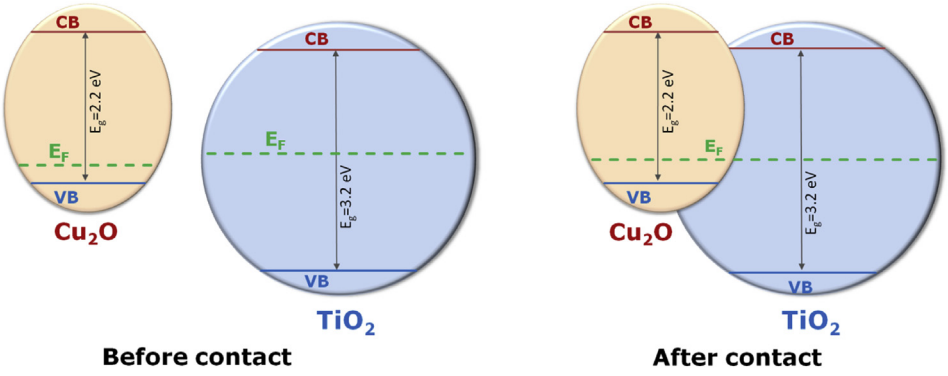

Fig. 1 – Energy band diagram of Cu_2O and TiO_2 before and after contact [45].

reduction deposition method. Typically, a fixed amount of MTA was dispersed in a Cu (II) nitrate ethanol solution, which was subsequently stirred at 40 °C. Reduction of Cu(II) on MTA surface was performed by suspending the Cu/TiO_2 composites into an aqueous solution containing glucose and NaOH. The resulting mixture was then stirred for at 60 °C, filtered, and the deriving solid was dried at 60 °C. HR-TEM images and XRD spectra clearly showed the presence of Cu_2O nanocrystals on the MTA surface. A rigorous comparison among the photocatalytic performances of the systems above described is not possible due to the different operating conditions employed (i.e. sacrificial organic agent, irradiation type, co-catalyst. etc). However, by simply comparing the values of hydrogen production rate per unit mass of photocatalyst, the best result between Cu_2O/TiO_2 composites prepared via glucose-based reduction method was recorded by Cheng et al. [68]. The Authors employed Cu_2O-decorated mesoporous TiO_2 beads (Cu_2O/MTBs) for methanol photoreforming by means of 400 W high-pressure mercury lamp without any UV cut-off filter and collected a maximum value of hydrogen production rate per unit mass of photocatalyst equal to 223 mmol/h g. Cu_2O/MTBs samples showed significantly higher (4.4–5-fold) evolution rates than P25–TiO_2.

Hydroxylamine

Zhen et al. [69] prepared Cu_2O/TiO_2 catalysts using selective reduction by hydroxylamine under alkaline conditions. More in detail, fixed amount of $CuCl_2$ and sodium dodecyl sulfate were added to deionized water containing P25–TiO_2. After adding NaOH to the aqueous mixture, a light blue suspension containing a Cu $(OH)_2$ precipitate was observed. Finally, NH_2-OH·HCl was quickly added into the suspension. After stirring, the mixed solution was kept at 30 °C for the growth of the Cu_2O crystals. The resulting orange solid was collected by centrifugation, followed by washing and drying in a 50 °C vacuum oven. Various samples with different loading amounts of Cu_2O on TiO_2 were prepared according to the same procedure and successively added to an aqueous mixture containing Eosin-Y and triethanolamine (TEOA). The mixed solution was then irradiated with visible light to prepare Cu/Cu_2O/Cu/TiO_2 composite photocatalysts through *in situ* photoreduction. The presence of Cu_2O was confirmed by XPS spectra, XRD spectra, and HR-TEM images. The Authors obtained a photoefficiency value expressed as Apparent Quantum Efficiency of about 45% at 520 nm, corresponding to a value of hydrogen production rate per unit mass of photocatalyst equal to 3.94 mmol/h g. Such highest value of hydrogen production rate per unit mass of photocatalyst reached almost 196 times that recorded over bare P25–TiO_2 and 3 times that of a reference Cu^0/TiO_2 sample.

Hydrazine

Zhu et al. [70] reported the formation of Cu_2O/TiO_2 nanotube-array heterogeneous structures by coating Cu_2O nanoparticles onto titanium dioxide via multiple-cycle chemical adsorption plus reduction method (MC-CAR). At first, TiO_2 NTAs were immersed into an aqueous solution containing $CuSO_4$ and glucose to ensure adequate absorption. TiO_2 NTAs were then soaked with deionized water to remove excessive $CuSO_4$.

Subsequently, the coated TiO_2 NTAs substrates with Cu^{2+} monolayer were dipped into a different aqueous mixture containing N_2H_4 and NaOH, in which Cu^{2+} was reduced to Cu_2O monolayer. The reduction process was again followed by soaking with deionized water. All such procedures were performed at 40 °C in a thermostatic bath. The resulting Cu_2O/TiO_2 composite materials were then dried at 100 °C in nitrogen atmosphere. The presence of Cu_2O clearly resulted from XRD spectra.

For photoelectrocatalytic hydrogen evolution experiment, Cu_2O/TiO_2 NTAs was used as the photoanode in a Na_2SO_4-ethylene glycol electrolyte solution. The photoanode was subjected to continuous irradiation under illumination intensity of 100 mW/cm^2 by a solar simulator coupled to an AM 1.5G filter. The highest photoefficiency value collected was equal to 6.2 mmol/h cm^2, which was 2.5 times that of TiO_2 NTAs (pure anatase phase).

Thiosulfate

Le et al. [71] obtained Cu_2O/TiO_2 nanorod arrays (TNA) through a growth method based on cyclic impregnation. In particular, two samples of TNA film on fluorine doped tin oxide glass substrates were immersed into four distinct solutions (i.e. 0.1 M $CuSO_4$ and 0.1 M $Na_2S_2O_3$ mixture, highly purified water, 0.1 M NaOH and highly purified water) for 5 s sequentially. The immersing process was repeated for 10 or 30 cycled times, respectively. At the end of this sequence, the two samples

Table 1 – Several articles on Cu_2O/TiO_2 composite materials.

I	II	III	IV	V	VI	VII	VIII	XI
Preparation method	Cu_2O identification technique	H_2 generation mechanism	TiO_2 type	Co-catalyst	Sacrificial agent	Lamp filter	Efficiency of H_2 generation	Reference
TNTs by hydrothermal method; copper modified TiO_2 by impregnation method	PL, XRD	p-n heterojunction	Home prepared	None	Glycerol	Direct sunlight between 10 a.m. and 3 p.m.	Not reported, best hydrogen evolution rate 48 mmol/h g	[84]
TiO_2 thin films deposited on quartz glass by electron beam evaporation at T = 200 °C; Cu_2O layers grown by laser ablation	XPS, XRD	p-n heterojunction	TiO_2 thin film	None	None	None (300 W Xenon lamp)	Not reported, highest H_2 production 2.76 10^{-3} mmol under UV light after 6 h	[128]
TiO_2 by hydrothermal method; CuO_x by wetness impregnation method and calcination at T = 400 °C at in air	DRIFTS, DRUV, HRTEM, XPS, XRD	p-n heterojunction	Anatase	None	Methanol	None (300 W Xenon simulated solar light)	Not reported, highest H_2 production 0.621 mmol/h g	[85]
Copper foam-based nanodots composites prepared by immersion-heating procedure and calcination at 300 °C	HRTEM, XPS, XRD	p-n heterojunction; Fermi levels formation	Not specified	CFE (Copper foam-based nanodots composite)	None	None	HER onset potential: 18 mV, potential: 114 mV and 10 mA/cm^2	[65]
Cu_2O/TiO_2 catalysts prepared by the alcohol-thermal method	EDX, ICP-OES, STEM–EDS, XPS, XRD	p-n heterojunction	Home prepared	None	Methanol	Cut-off filter $\lambda > 420$ nm (300 W Xenon lamp)	Not reported, highest H_2 production 24.84 mmol/h g	[118]
Three different preparation methods: Impregnation and calcination at T = 350 °C; Microwave reduction method and several washing with ethanol; Photodeposition method	PL, Raman, TEM, XPS, XRD,	Not reported	Commercial TiO_2 P25	None	Methanol	Sun condition	Not reported, highest H_2 production 0.891 mmol/h)	[86]
Electrodeposition method for Cu_2O film synthesis; $Au/Cu_2O/TiO_2$ electrode fabricated by dip-coating method; $Au/Cu_2O/TiO_2/WS_2$ photocathode fabricated by stirring, centrifugation, and washing procedure	XRD	p-n heterojunction; Fermi levels formation	Not specified	WS_2	None	Cut off filter ($\lambda \geq 420$ nm) (Xenon lamp- Light intensity 100 mW/cm^2)	Not reported, best photocurrent obtained was 10 mA/cm^2 at over-potential of −0.33 V vs RHE under visible light	[72]
TiO_2/Cu_2O core/shell NWAs prepared by hydrothermal method and chemical bath deposition	EDS, HRTEM, XPS, XRD	p-n heterojunction; Fermi levels formation	Rutile	None	None	None (300 W Xenon lamp- Light intensity 100 mW/cm^2)	Not reported, best photocurrent obtained was 2.50 mA/cm^2, with H_2 production 32 mmol/h cm^2	[127]
Bismuth modified TiO_2 prepared by sol-gel method; impregnation of copper on bismuth deposited TiO_2 and calcined at T = 400 °C	DRUV, FESEM, XPS, XRD,	Bi_2O_3 minimizes electrone-hole recombination	Commercial TiO_2 P25	Bi_2O_3	Glycerol	Solar simulator (300 W Xenon lamp- Light intensity 40 mW/cm^2)	Not reported, highest H_2 production 3.678 mmol/h	[105]
Cu_2O nanowires prepared by deposition method and coating of a layer of Cu_2O onto Cu_2O nanowire by electrodeposition; TiO_2 coating by deposition method	Raman, XRD	Not reported	Amorphous	RuOx-Ga_2O_3	None	Solar simulator (300 W Xenon lamp- Light intensity 100 mW/cm^2)	solar-to-hydrogen conversion efficiency ~3%	[76]

(*continued on next page*)

Table 1 – (*continued*)

I	II	III	IV	V	VI	VII	VIII	XI
Preparation method	Cu_2O identification technique	H_2 generation mechanism	TiO_2 type	Co-catalyst	Sacrificial agent	Lamp filter	Efficiency of H_2 generation	Reference
Cu(II)/TNT by impregnation and heating at T = 200 °C	XRD	p-n heterojunction	Home prepared	None	Glycerol	1.5 a.m. solar irradiance of white light (1000 W Hg/Xe-Light intensity 100 mW/cm^2)	Not reported, best photocurrent obtained was 3.40 mA/cm^2 with H_2 production 0.127 mmol/h cm^2	[89]
Cu_2O sheets prepared by thermal oxidation of thin copper foils; Ga_2O_3 and TiO_2 layers deposition by thermal atomic Layer deposition system; RuO_x prepared by photoelectrodeposition	XRD	Not reported	Not specified	Ga_2O_3/RuO_x	None	AM 1.5 G filter	1.75% at 0.5 V over Au/Cu_2O/Ga_2O_3/TiO_2/RuO_x; 1.9% at 0.45 V over Dual Cu_2O-based photocathodes	[49]
Cu_2O sensitized TNAs fabricated by cyclic impregnation growth method	XPS, XRD	Not reported	Home prepared TNAs	None	Glycerol	Cut off filter λ > 400 nm (300 W Xenon Lamp)	Not reported, highest H_2 production 4.8 10^{-4} mmol/h cm^2	[71]
nanoclusters prepared by green microwave-assisted method with glucose or onion skin waste	DRUV, FESEM, PL, Raman, TEM, XPS, XRD	p-n heterojunction	Commercial TiO_2 P25	None	Glycerol	Not reported (400 W metal halide lamp)	Not reported, highest H_2 production 4.70 mmol/g after 24 h	[66]
Cu_2O grown on Au/Cr/FTO/Glass substrate by potentiostatic electrodeposition; Cu_2O film coated with graphene and TiO_2 layers by atomic deposition; Pt loaded on all the devices	Raman, XPS, XRD	Not reported	Anatase	Pt	None	AM 1.5 G Solar simulator (Light intensity 100 mW/cm^2)	Not reported, best photocurrent obtained was −3 mA/cm^2 at 0.0 V vs RHE	[77]
Cu_2O film fabricated by electrochemical deposition on copper substrate; The Cu_2O/Au film prepared by photodeposition; Cu_2O/TiO_2 and Cu_2O/Au/TiO_2 films prepared by painting TiO2 solution onto Cu_2O or Cu_2O/Au films	DRUV, PL, SEM, TEM, XPS, XRD	Z-scheme system	Commercial TiO_2 P25	Au	Methanol, glucose	Cut off filter (300 W Xenon lamp)	Not reported, highest H_2 production *0.0125 mmol/cm^2	[78]
Cu/Cu_2O/Cu/TiO_2 prepared by selective reduction with hydroxylamine	DRUV, FESEM, HRTEM, PL, Raman, SEM, TEM, XRD	p-n heterojunction	Commercial TiO_2 P25	Cu/Eosyne	Triethanolamine	Cut-off UV filter (300 W Xenon lamp-Light intensity 100 mW/cm^2)	AQE = 45.7% at 520 nm	[69]
A Cu_2O film prepared by electrochemical deposition on copper substrate and coating with TiO_2	XPS, XRD	Not reported	Commercial TiO_2 P25	None	Methanol	UV-B and UV-C cut-off AM 1.5 filter (Xenon lamp-Light intensity 78 mW/cm^2)	Not reported, highest H_2 production 12.70 mmol/L	[79]
Cu−TiO_2 photocatalysts prepared by Sol-gel method	TPR, XPS, XRD	Not reported	Home prepared Anatase/Brookite	None	Ethanol	None	Not reported, highest H_2 production 3.865 mmol/h g	[129]
The Cu_2O films were synthesized by electrodeposition method	DRUV, FESEM, XPS, XRD	Not reported	Not specified	Cu	None	Cut off filter AM 1.5 (300 W Xenon-Light intensity 100 mW/cm^2)	Not reported, best photocurrent obtained was −2.04 mA/cm^2 at 0 V vs RHE	[80]
TiO_2−MOF-199 composite prepared by hydrolysis; Cu/Cu_2O over TiO_2 by calcination	DRUV, HRTEM, PXRD, XPS	p-n heterojunction and shifting of the Fermi level due to the presence of Cu nanoparticles	Anatase	Cu	Glycerol	None (100 W UV lamp-λ = 365 nm)	Not reported, highest H_2 production 15.13 mmol/h g	[110]

Hydrogen titanate nanotubes prepared by hydrothermal method; CuO_x/TiO_2 composite prepared by impregnation method and calcination at T = 400 °C	HRTEM, H2-TPR, XPS, XRD	p-n heterojunction	Anatase, Rutile, Brookite, P25	None	Methanol	None (300 W Solar simulator)	Not reported, highest H_2 production 3.203 mmol/h g	[87]
Cu–TiO_2 thin films deposited on quartz glass substrates by RF reactive magnetron sputtering	XPS, XRD	p-n heterojunction and the Fermi levels formation	Anatase	None	Methanol	None (300 W Xenon lamp)	Not reported, highest H_2 production 2.80 10^{-3} mmol/h cm^2	[119]
Cu-loaded photocatalyst prepared by impregnation and calcination	XPS	Cu_2O injects additional photoexcited electrons into the TiO_2 CB, thus TiO_2 produces hydrogen	Commercial TiO_2 P25	CuO	Glycerol	400 nm UV cut-off filter/300 W Xe lamp	Not reported, highest H_2 production 2.240 mmol/h g under UV–Vis light and 0.100 mmol/h g under visible light	[92]
TiO_2 nanotubes fabricated by electrochemical anodization; Cu_2O-doped TNAs prepared by square wave voltammetry electrochemical deposition method	SEM, XPS, XRD	p-n heterojunction; Fermi levels formation	Anatase	None	None	None (100 W Hg lamp)	Not reported, highest H_2 production 300 μM/cm^2 after 4 h and photocurrent obtained was 4.50 mA/cm^2 under bias potential of 1 V	[81]
CuO_x/TiO_2 thin films on quartz glass substrates prepared at T = 450 °C by RF reactive magnetron sputtering	XPS	Not reported	Anatase	CuO	Methanol	None (300 W Xenon lamp)	Not reported, highest H_2 production *5.30 10^{-3}mmol/h cm^2	[93]
Metal oxide cluster modified TiO_2 nanoplates prepared by hydrothermal method	XPS, XRD	Not reported	Home prepared	None	Methanol	Cut-off filter 250 nm < λ < 380 nm (300 W Xenon lamp)	Not reported	[130]
TiO2–Cu2O NWA grown on FTO glass substrate by hydrothermal synthesis	FESEM, HRTEM, TEM, XPS, XRD	Not reported	Home prepared	None	None	No filter (300 W Xenon lamp)	0.71%, photocurrent density (bias) obtained was 4.66 mA/cm^2	[18]
Cu_xO/TiO_2 composite prepared by impregnation method and calcination at T = 350 °C	DRUV, PXRD, Raman, XPS	p-n heterojunction	Home prepared TiO_2, Commercial TiO_2 P25 for comparison	Cu	Ethylene glycol-Propanol, ethanol, methanol for comparison	Sun condition Light intensity 1.15 10^5lx,	Not reported, highest H_2 production 79.80 mmol/h g	[88]
Cu_2O photocathode by electrodeposition method on FTO substrates; TiO_2 stabilization layers on Cu_2O photocathodes by ELAMOD process	XRD	Not reported	Home prepared	None	None	Cut off filter 420 nm (ABET Solar Simulators)	Not reported	[82]
Cu-loaded TiO_2 catalysts obtained by chemical reduction deposition method	DRUV, EDS, HR-TEM, NIR, XRD	p-n heterojunction	Home prepared	Cu	Methanol	Cut off filter 360 nm <λ < 780 nm Or λ > 420 nm (300 W Xenon lamp)	AQE = 13.5% at 365 nm	[67]
Cu_2O coating layer deposited onto TiO_2 tube walls by multiple-cycle chemical absorption and reduction method	EDX, XRD	p-n heterojunction; Fermi levels formation	Home prepared	None	Ethylene glycol	AM 1.5G filter (Solar simulator- Light intensity 100 mW/cm^2)	Not reported, highest H_2 production *6.2 mmol/h cm^2	[70]

(continued on next page)

Table 1 – (*continued*)

I	II	III	IV	V	VI	VII	VIII	XI
Preparation method	Cu_2O identification technique	H_2 generation mechanism	TiO_2 type	Co-catalyst	Sacrificial agent	Lamp filter	Efficiency of H_2 generation	Reference
Cu_2O microcrystals obtained with autoclaves, heating, precipitation, washing and distillation method	EPR, XRD	Electron-hole pair formation or reduction of formaldehyde and capture of oxygen from Cu_2O	None (commercial TiO_2 P25 as reference)	None	Formaldehyde	Cut off filter $\lambda \geq 420$ nm (Xenon lamp-Light intensity 50 mW/cm^2)	Not reported, highest H_2 value 82.2 μmol after 3 h	[131]
Cu/TiO_2 photocatalysts prepared by photoreduction method	None	Cu/TiO_2 NPs absorbs the whole range of visible light	Commercial TiO_2 P25	None	Glycerol	Cut-off filter $\lambda \geq 420$ nm (500 W Xenon lamp- Light intensity 1.5 mW/cm^2)	Not reported, highest H_2 production 0.24 mmol/h g	[120]
Cu modified TiO_2 nanorods prepared by wet-impregnation method	None	Electron-hole pair formation	Home prepared	None	Glycerol	Direct sunlight	Not reported, highest H_2 production 0.0503 mmol/h g	[3]
Not reported, photoreduction of Pt on the catalyst surface	None	Cu_2O as antenna capturing the radiation, electrons are transferred from CB of Cu_2O to Pt	Not specified	Pt	Methanol	None (Tungsten lamp)	Not reported, highest H_2 production *1.82 mmol/h g	[113]
Cu_2O/TiO_2 nanotube arrays prepared by electrochemical deposition method	None	Not reported	Home prepared	None	None	AM 1.5 G solar simulator (100 mW/cm^2)	Not reported	[132]
The Cu_2O/TiO_2 photocatalysts prepared by reduction method	DRUV, XPS, XRD,	p-n heterojunction	Commercial TiO_2 P25	None	Methanol, ethanol, glycerol, ethylene glycol	None (500 W Xenon lamp)	AQE = 4.32%	[74]
The Cu_2O–TiO_2 photoelectrodes prepared by spray pyrolysis process and sputter coating of thin layer of TiO_2	XPS	Not reported	Not specified	None	Glucose	Not reported	Not reported highest H_2 production ~0.122 mmol/h cm^2	[133]
Cu_2O/TiO_2 particles prepared by glucose solvothermal method	AES spectra, HRTEM, XPS, XR	Similar mechanism to Z-scheme	Commercial TiO_2 P25	None	Ethanol	None (300 W Xenon lamp)	Not reported, highest H_2 production 0.668 mmol/h g	[60]
Mesoporous TiO_2 beads produced by metal-salt based hydrothermal process; Cu_2O-decorated mesoporous catalysts prepared by chemical bath deposition process	XPS, XRD	The Cu_2O nanocrystals as electron-hole separation centre	Home prepared	None	Methanol	None (400 W high-pressure Hg lamp)	Not reported, highest H_2 production 223 mmol/h g	[68]
The Cu_2O/TNA composites obtained by electrochemical deposition of Cu_2O in a three-electrode cell	XRD	p-n heterojunction	Home prepared	None	Glycerol	Cut-off filter (Xenon lamp)	Not reported, highest H_2 production 8.9 mmol/h cm^2	[83]

The Cu_2O grid deposited on TiO_2 thin films by microsphere lithography strategy and Pt addition by deposition method	GIXRD	Not reported	Home prepared	Pt	Methanol	None (Xenon lamp)	Not reported, highest H_2 production 0.06 mmol/h	[134]
Cu_2O on titania nanotubes by electrodeposition method	XRD	Not reported	TiO_2 nanotubes	None	None	Cut-off filter $\lambda > 500$ nm (TS428 lamp 350 nm $< \lambda <$ 2500 nm)	Not reported	[73]
Cu_2O/TiO_2 composite prepared by ethanol-induced deposition method and calcination at T = 350 °C	HR-TEM, XPS, XRD	p-n heterojunction	Commercial TiO_2 P25	None	Ethylene glycol	None (Xe lamp 320 nm $< \lambda <$ 780 nm)	AQE = 28.6% at 365 nm	[59]
Cu_2O through chemical reduction with ascorbic acid; Au deposition through photo reduction process	XRD, XPS	p-n heterojunction and SPR of Au	Home prepared TiO_2 nanorods	Au	Ethanol	AM 1.5 G filter (300 W Xenon lamp)	Not reported, highest H_2 production 8.548 mmol/h g	[135]
The Cu_2O-TiO_2 prepared by self-assembly approach in presence of AOT except that the addition of TiO2. After stirring for 3 h, the solution was kept at 80 °C for 4 h, then centrifuged, washed and dried.	XRD, XPS	p-n heterojunction	Home prepared TiO_2	None	Methanol	300 W Xe lamp	Not reported, highest H_2 production 0.5 mmol/h g	[114]
Cu_2O prepared by oxidation of Cu^0 in 6 h. Au $-Cu_2O$ prepared by partial galvanic replacement reaction. Mixing of Cu_2O or $Au-Cu_2O$ with TiO_2, deposition onto a glass substrate dipped in isopropanol for 10 min, cleaned through plasma for 10 min and drying in oven at 100 °C for 15 min.	TEM, SEM, Raman, XPS, UV–Vis absorption, ICP	p-n heterojunction	Anatase	Au	Ethylene glycol	Cut-off filter $\lambda > 360$ nm (100 W UV lamp-8 mW/cm^2); Cut-off filter $\lambda > 430$ nm (300 W Xe lamp)	Not reported, highest H_2 production 12 mmol/h g	[57]
Cu_2O-TiO_2 prepared by sol-gel method; after illumination Cu doped $TiO_2$was reduced to Cu_2O-TiO_2.	BET, EDX, TEM, SEM, XRD, DRUV-Vis, Raman, EPR, PL	Reduction of Cu to Cu_2O and p-n heterojunction	Isopropyl titanate	None	Methanol	None (300 W Xe lamp)	Not reported, highest H_2 production 16.25 mmol/h g	[106]
Cu_2O and Cu_2O/TiO_2 photocathodes prepared by electrodeposition of Cu_2O and deposition of titanium tetrapropoxide. The rGO/NiFe-LDH composite catalyst was synthesized by hydrothermal method. Cu_2O/TiO_2/rGO/NiFe-LDH photocathodes prepared by dip-coating method.	XRD, FESEM, SEM, XPS, Raman, R, DRUV–vis	p-n heterojunction	Titanium tetraisopropoxide	rGO/NiFe	0.5 M Sodium sulfate	AM 1.5 G solar simulator (100 mW/cm^2)	0.41% at 0.25 V vs RHE	[75]
Cu_2O/TiO_2 prepared by magnetron sputtering method; The deposition temperature was 550 °C for 12 h, obtaining TiO_2 arrays. Deposition of CuO_x by sputtering copper, with controlled flow rate of oxygen.	XRD, XPS, AES	Enhanced performance attributed to metallic Cu, produced during the irradiation	Anatase	None	Methanol	None (300 W Xe lamp - 300 nm $\leq \lambda \leq$ 2500 nm)	Not reported, highest H_2 production 3.7 10^{-3}mmol/h cm^2	[117]

(continued on next page)

Table 1 – (continued)

I	II	III	IV	V	VI	VII	VIII	XI
Preparation method	Cu_2O identification technique	H_2 generation mechanism	TiO_2 type	Co-catalyst	Sacrificial agent	Lamp filter	Efficiency of H_2 generation	Reference
TiO_2 nanostructures via hydrothermal method, followed by thermal reduction strategy, at 300 °C for 2 h with H_2 flow. Copper-related species were deposited onto TiO_2 via photodeposition route.	XPS	Z-scheme Cu_2O/TiO_2	Anatase	Pt	Methanol	Monochromatic light (350 nm) with filter (300 W Xe lamp)	53.5% at 350 nm	[116]
The (001) TiO_2@ $Ti_3C_2T_x$ was prepared by a hydrothermal method. The Cu_2O/(001) TiO_2@ $Ti_3C_2T_x$ hybrids were synthesized via a modified solvent reduction method.	XRD, TEM, XPS, AES, DRUV-Vis	Migration and spatial separation of photogenerated charge carriers among $Ti_3C_2T_x$, TiO_2, and Cu_2O	Anatase	$Ti_3C_2T_x$	Methanol	None (300 W Xe lamp)	Not reported, highest H_2 production 0.612 mmol/h g	[115]

were dried at the atmosphere. Cu 2p XPS spectra before and after HER upon a Xe lamp irradiation with UV cut off filter demonstrated the presence of Cu_2O on the catalyst surface.

As regards the best photocatalytic activity for hydrogen evolution found by using this method, a maximum photoefficiency value of about 4.8 10^{-4} mmol/h cm^2 was recorded by adopting glycerol as sacrificial organic species and a 300 W Xenon Lamp endowed with a UV-cut off filter ($\lambda > 400$ nm). Such maximum photoefficiency for hydrogen evolution was about 4-fold higher than that of pure TNAs (rutile phase).

Electrochemical deposition

As shown in Table 1, Column I, electrochemical deposition method was adopted by plenty of authors in the literature survey to prepare Cu_2O/TiO_2 composites for photocatalytic hydrogen evolution [49,72–83], most of whom employed Cu_2O/TiO_2 as an effective and low-cost photocathode material in photoelectrochemical cells.

Zhang et al. [83] employed a three-electrode system to fabricate a film made of TiO_2 nanotube arrays, which was used as working electrode. A Pt mesh and an Ag/AgCl electrode were employed as auxiliary and reference electrodes, respectively.

A suitable electrolyte was prepared by dissolving a fixed amount of $CuSO_4$ in a lactic acid solution, whose pH was adjusted by adding proper quantities of NaOH. Electrodeposition charges of 500 mC were applied on the stirred electrolyte during the deposition process. Different types of Cu_2O/TNA samples were synthesized by varying the deposition potential applied vs Ag/AgCl. The obtained samples were then dried at 50 °C in vacuum. SEM images, as well as XRD spectra, revealed the presence of octahedral Cu_2O particles on the TNA surface. The best photocatalytic performances were obtained by using methanol as sacrificial agent and a light source (Xenon lamp) with a UV cut-off filter. In such conditions, 8.9 mmol/h cm^2 of hydrogen were produced, indicating a remarkable activity of the electrode employed. Such maximum photocatalytic hydrogen evolution rate recorded over Cu_2O/TNA photocatalyst was about 42 times higher than pure TNA (mixed anatase-rutile phase).

Impregnation/calcination

Amongst most commonly adopted Cu_2O/TiO_2 preparation techniques, wet impregnation followed by calcinations should be definitely mentioned. Impregnation was used in several studies from the literature survey to merge TiO_2 (i.e. commercial or home prepared) and Cu_2O nanoparticles, always followed by calcination under various temperature and atmosphere conditions and for different treatment times [84–89].

Liu et al. [87] prepared Cu_2O/TiO_2 photocatalysts employing TiO_2 with different phase structures as well as P25 as supports via an incipient wetness impregnation/calcinations method. More in detail, a fixed amount of TiO_2 (i.e. commercial P25 or anatase, rutile, and mixed phases of anatase/rutile/brookite prepared via hydrothermal method) was impregnated with appropriate quantity of $Cu(NO_3)_2$ in aqueous solution at room temperature, and was then dried

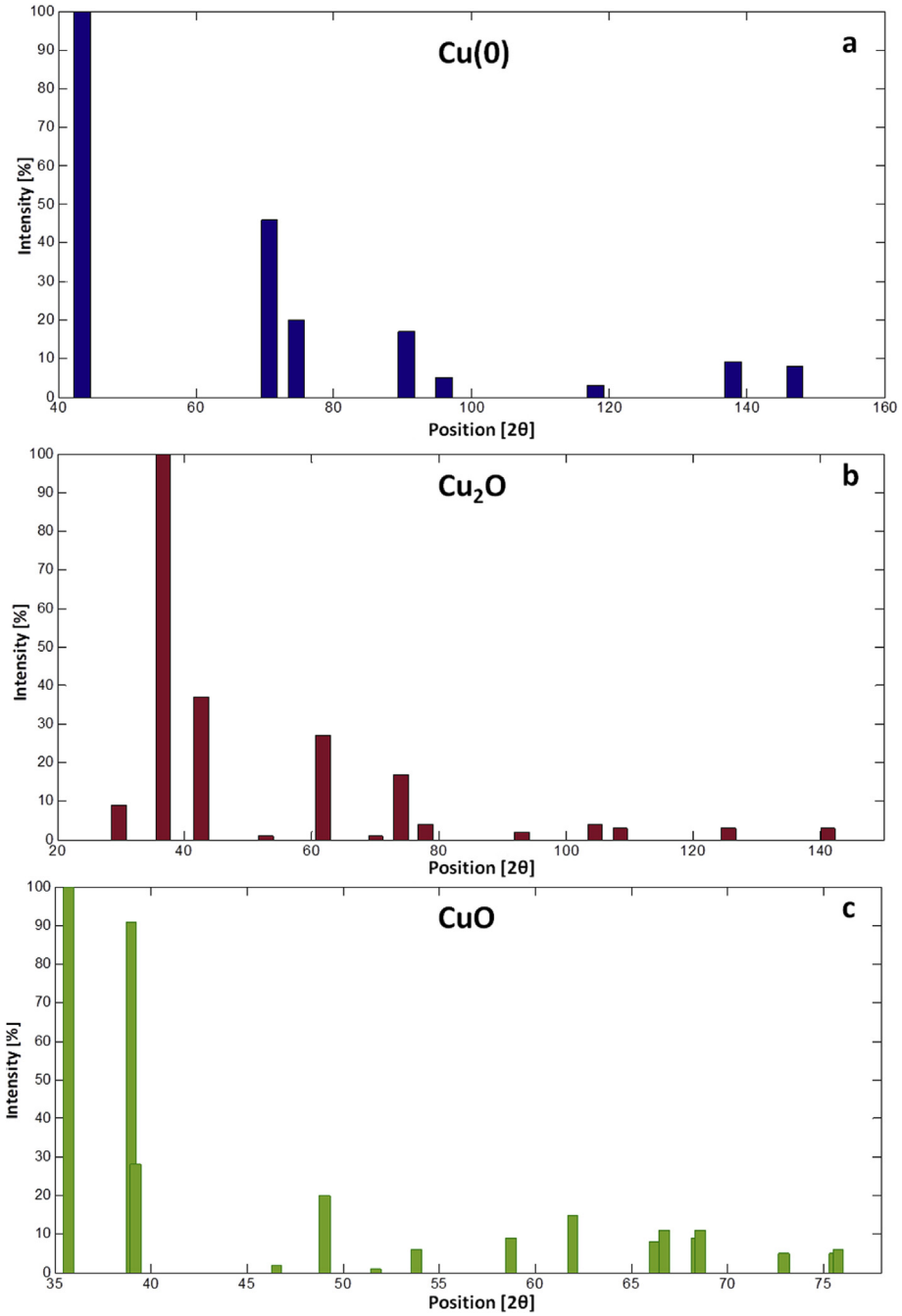

Fig. 2 – XRD signals of Cu(0) (a), Cu_2O (b), and CuO (c).

at 100 °C. The resulting powder was successively calcined at 400 °C in air. XPS spectra, as well as HR-TEM images and H_2-TPR profiles revealed the presence of cuprous oxide on the surface of the titania supports with various crystalline phase composition.

Dubey et al. [89] employed a wet chemical treatment to obtain Cu_2O/TiO_2 nanostructures by using crystallized aligned TiO_2 nanotubes (TNTs) and a solution containing $Cu(NO_3)_2$ and NaOH. For a typical preparation procedure, fixed amounts of Cu $(NO_3)_2$ and crystalline aligned TNTs were suspended and stirred in aqueous solution. NaOH was then added dropwise to such suspension at varying molarities. These samples were successively washed with alcohol and dried through an air stream, and then heated at 200 °C. Cu_2O formation was confirmed by XRD spectra, SEM images, and HR-TEM analyses. As concerns the photocatalytic performances of the as prepared Cu_2O/TiO_2 composites, a maximum value of hydrogen production equal to 79.8 mmol/h g was achieved by Praveen Kumar et al. [88] by adopting ethylene glycol as sacrificial organic agent under direct solar light irradiation with an average light intensity of 1.15 10^5 lx. The Cu_2O/TiO_2 photocatalyst prepared by Praveen Kumar et al. [88] exhibited

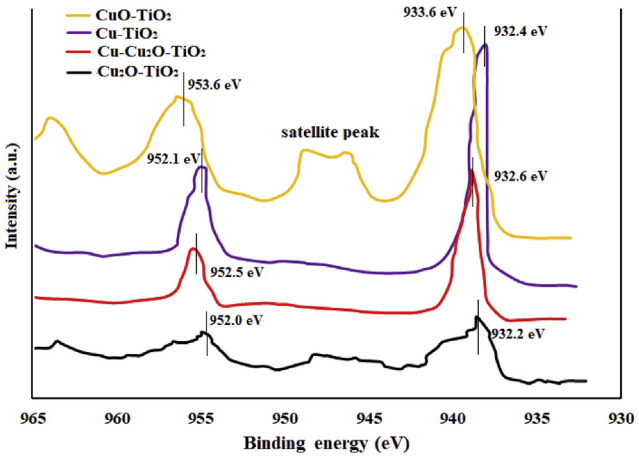

Fig. 3 – XPS spectra of $Cu/Cu_2O/Cu/TiO_2$, Cu/TiO_2, Cu_2O/TiO_2, and CuO/TiO_2 adapted by Zhen et al. [49]: (1) CuO/TiO_2; (2) Cu/TiO_2; (3) $Cu/Cu_2O/Cu/TiO_2$; (4) Cu_2O/TiO_2.

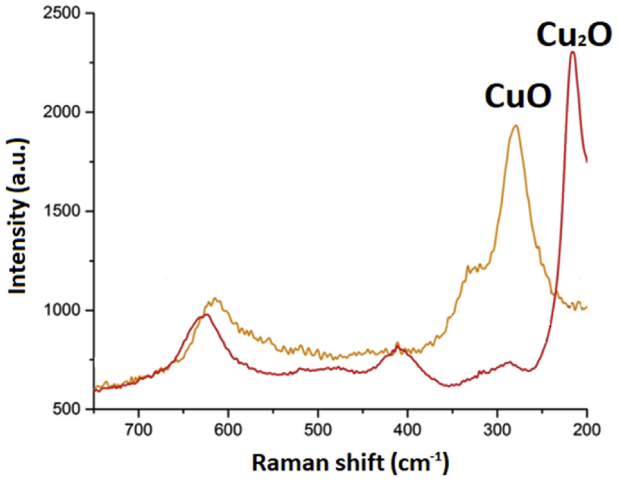

Fig. 4 – Raman spectra of CuO and Cu_2O.

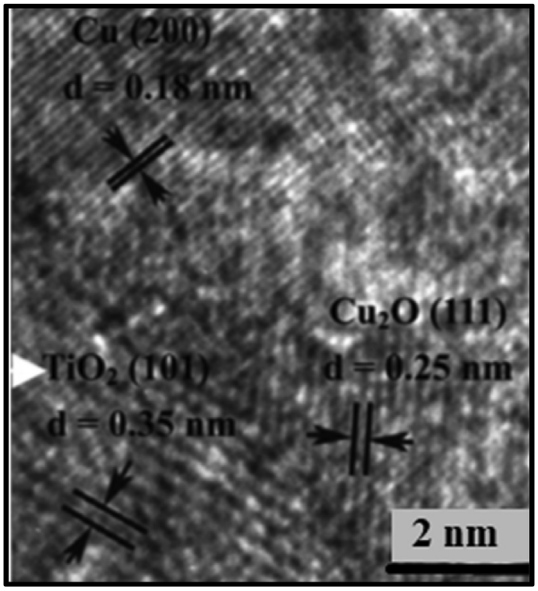

Fig. 5 – HRTEM of Cu_2O in Cu_2O/TiO_2 composite [84].

enhancements of 33 and 18 fold in hydrogen production rate as compared to commercial P25–TiO_2 nanoparticles (TNP) and calcined TNTs, respectively.

In conclusion of this paragraph, it can be stated that, irrespective of the preparation method, Cu_2O/TiO_2 composite photocatalysts prepared as above reported are all capable of ensuring hydrogen production rates higher than bare P25–TiO_2 and sometimes under visible light irradiation only. In particular, the highest increase in reactivity was firstly observed for a Cu_2O/TiO_2 photocatalysts prepared through via reduction of cupric species by means of hydroxylamine. Significant results may be also obtained by the adoption of an electrochemical deposition method.

Characterization techniques for Cu_2O/TiO_2 composite materials

The main techniques adopted to characterize Cu_2O/TiO_2 composite materials are described hereafter. Two distinct classes of characterization are reported for such materials:

1) Characterization techniques devoted to the unique identification of the oxidation state of copper, which is deposited on the photocatalyst surface and responsible for the co-catalytic activity. X-ray diffraction spectroscopy (XRD), X-ray photoelectron spectroscopy (XPS), Raman Spectroscopy, and High-resolution transmission electron microscopy (HR-TEM) belong in this category.
2) Characterization techniques aimed at evaluating the capability of such photocatalysts to (i) absorb irradiated light, with special attention to visible-light-responsive materials, and (ii) reduce the likelihood of charge carrier recombination. Diffuse Reflectance UV (DRUV) Spectroscopies and Photoluminescence (PL) belong in this category.

Copper species identification

XRD spectroscopy

XRD spectra signals can be used to univocally identify copper oxidation state on the photocatalyst surface through the knowledge of the spectra of the single oxidation state. To this aim, as shown in Fig. 2, XRD data recorded using an analytical method previously reported [90] indicate that:

i) The spectrum of Cu(0) presents the peaks corresponding to an angle 2θ [°] of 43.23, 50.51, 74.30 with d-spacing values [Å] of 2.09, 1.81, 1.28, respectively. These peaks are expected for a cubic form of metallic copper [91];
ii) The spectrum of Cu_2O is characterized by the presence of some peaks 2θ values [°] equal to 29.74, 36.65, 42.57, 52.80, 61.76, 70.06, 74.05, 77.89, 93.11, 104.60, 108.52, 125.56, and 141.22, with d-spacing values [Å] of 3.02, 2.4, 2.13, 1.74, 1.51, 1.35, 1.29, 1.23, 1.07, 0.98, 0.95, 0.87, and 0.82, respectively;
iii) For cupric oxide nanoparticles (CuO), the peaks found in the XRD spectrum at 2θ values [°] of 35.44, 35.49, 38.72, 48.65, with d-spacing values [Å] of 0.253, 0.252, 0.232,

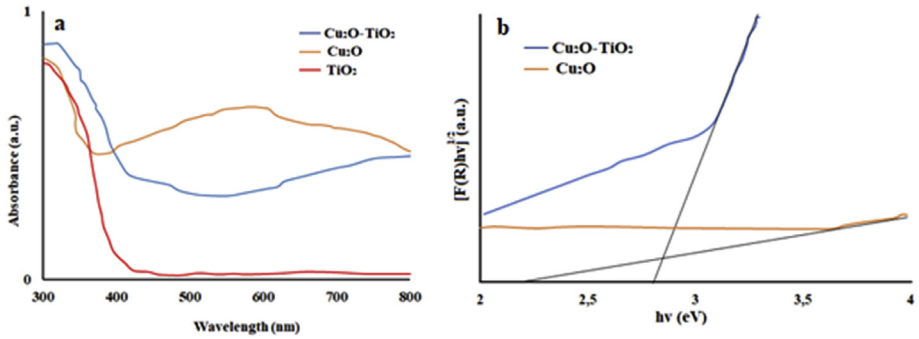

Fig. 6 – (a) Typical DRUV absorption spectra in presence of bare TiO_2, bare Cu_2O and Cu_2O–TiO_2 composite, and (b) plots of $(F(R)hv)^{1/2}$ versus photon energy hv for Cu_2O and Cu_2O–TiO_2 composite [46].

and 0.187, respectively, well agree with JCPDS data (JCPDS cards n. 65–2309).

XPS spectroscopy

The following remarks, matched with the spectra in Fig. 3 reported by Zhen et al. [69], may help to clearly identify the oxidation state of copper species on the photocatalyst surface by means of XPS. In CuO/TiO_2 The peaks at nearly 933.6 and 953.6 eV univocally indicate the presence of Cu(II) [69]. The double-peak between 940 eV and 945 eV is reported to be a Cu(II) satellite peak [69,76] but in the same position also Cu(I) showed a low satellite peak. On the other hand, the typical Cu(I) peaks of Cu_2O in Cu_2O/TiO_2 are individuated at 932.2 and 952.0 eV.

On the basis of the consideration reported above, an application of this technique was presented by Jung [92]: they indicated that most part of copper in air-calcined Cu/TiO_2 based photocatalysts is present in the form of Cu(II) with a peak at 934.1 eV, whereas a reduced presence of Cu(I) and Cu(0) is generally recorded (the presence of Cu (II) can be due to the oxidation of Cu (I) in air). On the other hand, when such photocatalytic materials are reduced under hydrogen atmosphere, an increase in intensity of the peaks related to Cu(I) and Cu (0) and a decrease in intensity of both Cu at 934.1 eV and satellite peaks are observed.

It is generally accepted that the similarity between the binding energies of Cu(I) and Cu(0) does not allow to unequivocally differentiate these two species and further spectroscopic indications are required (e.g. XRD, Raman, etc).

Raman spectroscopy

Limited literature information is available on Raman spectroscopy of Cu oxides [18,67,81,82,93]. Conflicting indications about the correlation between copper species and related peaks in Raman spectra are reported. Therefore, selected peaks providing a clear distinction between cupric and cuprous oxides were considered. More in details, the typical most intense Raman peaks corresponding to 216, 520, and 640 cm^{-1} are reported [94–96] for Cu_2O, whereas a peak at around 280 cm^{-1} is commonly attributed to the presence of CuO [94,95,97–100]. Some of the most intense peaks capable to unambiguously identify cupric and cuprous oxides obtained according to an analytical procedure previously reported [90] are shown in Fig. 4.

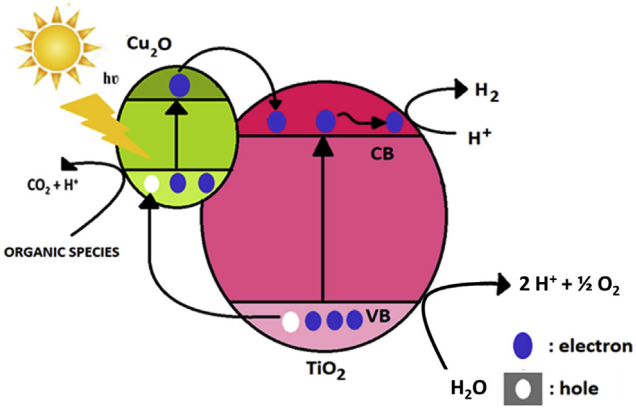

Fig. 7 – Schematic illustration for the hydrogen evolution reaction (HER) process over Cu/TiO_2 composite photocatalysts: oxidation of organic species (or water) by positive holes in the valence band and proton reduction by photogenerated electrons in the conduction band.

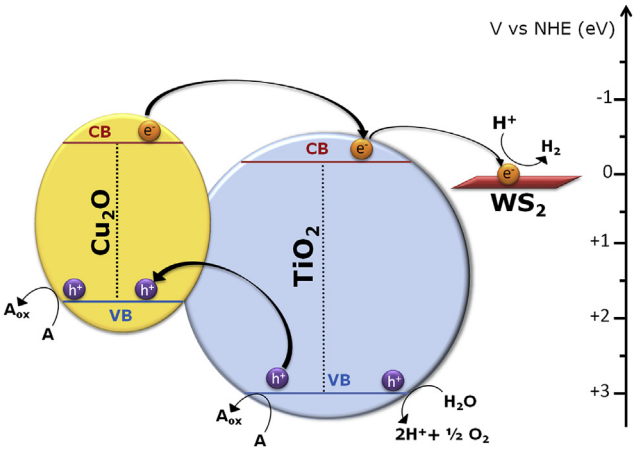

Fig. 8 – Schematic reaction mechanism of HER process over $Au/Cu_2O/TiO_2/WS_2$ photocathode proposed by Li et al. [52].

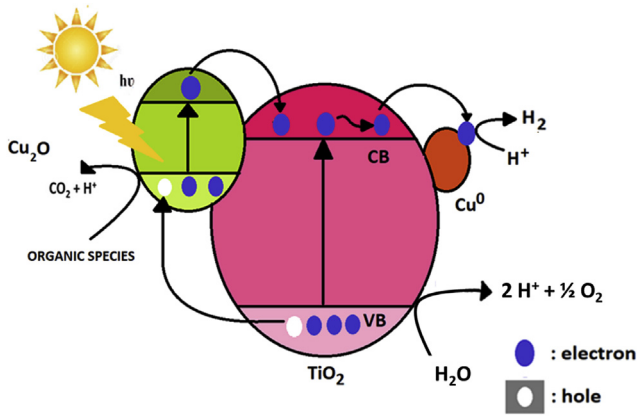

Fig. 9 – HER process over Cu (0)/Cu_2O/TiO_2/WS_2 composite photocatalysts under visible light irradiation.

HR-TEM

Several authors used HR-TEM analyses for structural and morphological characterization of Cu/TiO_2 composite materials, obtaining different results using commercial or home prepared TiO_2 as well as a different preparation method. HR-TEM images also allow to undoubtedly identify the Cu valence state in Cu-based TiO_2 photocatalysts for hydrogen evolution. In this regard, plane spacing values of nearly 0.25 and 0.28 nm corresponding to the d spacing of Cu_2O (111) have been reported [59,69,101,102] in Cu_2O/TiO_2 nanocomposites, as shown in Fig. 5. The presence of Cu_2O nanoparticles in Cu_2O/TiO_2 composites can be also clearly distinguished in TEM images by their peculiar structure, which is reported to have cubic shape [103]. On the other hand, as previously reported [102], the presence of CuO in Cu/TiO_2 nanocomposites could be distinguished through the existence of particles with rhombic shape in HR-TEM images. In general, the attribution of specific planes and their corresponding lattice spacings in HR-TEM images could give relevant information about the crystallinity grade and the morphology of Cu_2O/TiO_2 composites.

DRUV

Fig. 6(a) shows the typical UV–vis absorption spectra for pure Cu_2O and Cu_2O/TiO_2 composites, obtained according to an analytical method previously reported [90]. As concerns cuprous oxide, it exhibits a broad absorption band in the visible range from about 430 nm. The intensity recorded in UV–visible spectra maybe also indicated by the Kubelka–Munk function F(R). Fig. 6 (b) shows the energy gap value estimated through the linearization of Tauc plot of $(F(R)\ hv)^{1/2}$ versus photon energy (hv). The energy gap value resulting for Cu_2O (i.e. ≈2.2 eV) is consistent with other literature data [104]. Several authors [66,69,78,85,105] employed such diagnostic technique to evaluate the absorption property as well as the photocatalytic activity of Cu_2O/TiO_2 composite materials. As shown in Fig. 6 (a), they reported an increase in visible light absorption with respect to bare TiO_2 above 430 nm due to the presence of Cu_2O (as previously reported). In addition, a reduction in energy gap value (see Fig. 6 (b)) over Cu_2O/TiO_2 composite photocatalysts for hydrogen evolution was recorded.

PL

In photocatalysis, investigation on absorption/emission properties is essential to understand electronic interaction between composite materials and charge transfer mechanism for photocatalytic reactions. In order to gain a fully understanding on the electronic effect of copper species embedded as co-catalysts, photoluminescence studies on Cu_2O–TiO_2 materials have been performed by several authors in the literature review [66,69,78,84,86,106]. PL spectra of Cu_2O–TiO_2 photocatalysts revealed a decrease in photoluminescence intensity in with respect to bare TiO_2 [66,86], thus indicating that cuprous oxide lowers the recombination likelihood of photogenerated charge carriers. Indeed, the best photocatalytic performances in terms of hydrogen generation were commonly recorded over Cu_2O–TiO_2 samples showing the lowest PL intensity, as lower electron-hole recombination results in decreased light emission intensity, thus increasing photocatalytic efficiency [107].

Mechanisms of hydrogen evolution reaction

A reaction mechanism for p-n heterojunction based Cu_2O/TiO_2 materials attributes to cuprous oxide the role of energy antenna, due to its capability to absorb energy in the visible light spectral range. After charge carriers generation, it is reported that electrons in the conduction band (CB) of Cu_2O, due to the difference in potential of the CB bands (i.e. −1.5 V versus NHE for Cu_2O and −0.5 V versus NHE for TiO_2 [108] are transferred firstly to TiO_2, and subsequently to proton ions which are reduced. At the same time, as shown in Fig. 7, photogenerated holes are consumed by the sacrificial organic species which oxidizes [87].

The possibility for $Cu(I)$ of being reduced to $Cu(0)$ species, according to reaction r_1, was also considered by some authors as a possible explanation for a decrease in H_2 evolution photoefficiency [67].

$$Cu(I) + e^- \rightarrow Cu(0) \quad r_1$$

On the other hand a prompt reoxidation of $Cu(0)$, by holes as expressed by reaction r_2, was proposed by studies reporting that the presence of $Cu(I)$ remains unchanged on photocatalyst surface during hydrogen evolution reaction (HER) [59,60].

$$Cu(0) + h^+ \rightarrow Cu(I) \quad r_2$$

However, it is noteworthy that such aspects are analyzed only in some of the studies considered in the present review, so that no conclusion can be actually drawn on the fate of Cu(I) on the TiO_2 surface upon irradiation.

The effects of selected co-catalysts, such as WS_2 [72], Pt [77], Bi_2O_3 [105] and Ga_2O_3 [49,109] on the performances of Cu_2O/TiO_2 materials for HER were also investigated, as reported in Table 1, Column V. It is reported that they essentially help enhance photogenerated charge carrier separation, thus reducing their likelihood of recombination.

As reported by Li et al. [72] for instance, the role of WS_2 nanosheets in an Au/Cu_2O/TiO_2/WS_2 composite photocathode for hydrogen evolution is that of accepting electrons for water

reduction rapidly, thus promoting the separation process of the electron–hole pairs for a higher photocurrent. As shown in Fig. 8, under visible light irradiation ($\lambda \geq 420$ nm), electrons of Cu_2O are excited and easily transferred first to the CB of TiO_2, and then to the WS_2 layer, as the CB of TiO_2 and the Fermi level of WS_2 are more positive than the CB of Cu_2O. Subsequently, protons from the electrolyte promptly react with electrons, thus releasing hydrogen on the WS_2 surface. On the other hand, it is considered that the Au layer in the Cu_2O-based photocathode only decrease the electrochemical impedance of the Cu_2O photocathode.

Metal copper is also reported to act as a cocatalyst in Cu(0)/Cu_2O/TiO_2 composites [67,69,80,88,110]. The double effect of (i) promoting charge carriers separation and (ii) improving visible light absorption and photoactivity due to the localized surface plasmon resonance (LSPR) of Cu nanoparticles is related to the presence of Cu(0) [67]. The mechanism of hydrogen evolution over Cu(0)/Cu_2O/TiO_2 has been schematically illustrated in Fig. 9.

As regards the effect of TiO_2 type on the reaction mechanism over Cu_2O/TiO_2 photocatalysts, it is significant to note that the use of home-prepared mesoporous TiO_2 is related to a remarkable enhancement in photoefficiency for hydrogen evolution [67,111]. Such positive effect has been mainly attributed to a reduced recombination of photogenerated charge carriers and an increase in the interfacial electron transport within the Cu_2O/TiO_2 heterojunction, thus resulting in enhanced photocatalytic hydrogen generation [67,111].

Effect of pH

Some of the Authors reported in a previous paper [28] that pH considerably affects photocatalytic hydrogen generation over copper-modified TiO_2 catalysts.

It is widely acknowledged that moderate alkaline conditions may result into a favorable environment for generating hydrogen, probably due to higher photocatalyst stability and absence of cupric ion release in the reacting solution. While not all studies considered pH as a key factor in HER, some results reported in the literature survey support the crucial role of pH in photocatalytic H_2 evolution over Cu_2O/TiO_2 composites.

Indeed, Zhen et al. [69] reported that the results collected during photocatalytic hydrogen generation over a ternary catalyst (i.e. Cu/Cu_2O/TiO_2) indicate an intense activity at pH values around 9.0. On the other hand, a decline in photoefficiency for higher and lower pH values with a standstill in H_2 generation for values smaller than 5.0 and greater than 13.0 was recorded. Under acidic conditions, such experimental findings were related to Cu_2O instability and sacrificial agent (i.e. triethanolamine) protonation. Instead, under alkaline conditions, extremely low proton concentration may considerably slow down hydrogen generation rate.

Effect of sacrificial agent

Despite the main purpose of the photocatalytic processes aimed to hydrogen production is water photosplitting [112], only few studies considered in this review reported the photocatalytic hydrogen production in the absence of organic species. In this respect, in the presence of Cu_2O/TiO_2 composite materials the effect of the sacrificial agent was evaluated. As reported in Table 1 Column VI, methanol [67,68,74,79,85,86,93,106,113–119] and glycerol [3,66,71,83,84,89,92,105,110,120] are the most widely used organics for photocatalytic hydrogen production.

Li et al. [74] reported the results in terms of hydrogen generation in the presence of several sacrificial agents, thus showing an enhancement in photocatalytic activity by reducing the C/OH ratio. Moreover, as reported by Li et al. [74], the scavengers react with hydroxyl radicals, thus resulting in enhanced activity in case of molecules with simplest structure.

Praveen Kumar et al. [88] compared the photocatalytic activity for H_2 evolution in the presence of different scavengers under natural solar light irradiation. Hydrogen production was enhanced with increasing alcohol polarity, due to the different surface properties of the photocatalyst obtained, as well as the adsorption and electron donation properties. Moreover, a great enhancement in hydrogen production was detected by using several organics, such as ethylene glycol, due to the position of its oxidation potential with respect to the valence band potential of titania.

Hydrogen generation efficiency

Only Cu_2O/TiO_2 materials exhibiting considerable efficiencies for H_2 production under visible light irradiation may be considered for industrial applications. Despite solar energy is a perennial energy source, several issues undermine the photoefficiency of such composites, such as the followings:

1) The recombination reaction seizes a portion of photogenerated charge carriers potentially available for HER;
2) The energy carried by the incident radiation is higher than the bandgap value (E_g), in which case excess energy is dissipated in the form of heath or light;
3) The energy carried by incident photons is lower than E_g, in which case no effective light absorption happens.

As reported in the sections below, different indicators may be used to quantify the efficiency of energy capture depending on the experimental setup adopted. Among the papers found in the literature survey, only a few of them reported data of hydrogen generation efficiency (see Table 1). Overall, this is one of the major weakness affecting literature on hydrogen generation through photocatalytic processes.

Photoelectrochemical cells

Dotan et al. [121] defined the solar to hydrogen (STH) conversion efficiency of photoelectrochemical solar cells according to Eq. (1), where e J_{sc} is the short-circuit photocurrent density, η_F the Faradaic efficiency for H_2 production, and P the incident irradiation power density. Such parameters should be estimated under standard solar irradiation conditions (AM 1.5 G),

without any sacrificial agents, and pH or electrical bias between counter and working electrodes.

$$STH = \left[\frac{\left|J_{sc}\left(\frac{mA}{cm^2}\right)\right| \times 1.23(V) \times \eta_F}{P\left(\frac{mW}{cm^2}\right)}\right]_{AM1.5G} \quad (1)$$

Pan et al. [76] developed a $Cu/Cu_2O/Ga_2O_3/TiO_2/NiMo$ photocathode with a coaxial nanowire structure based on Cu_2O/Ga_2O_3-buried p-n junction. Such Cu_2O-based photocathode was employed together with a $BiVO_4$ photoanode for unassisted solar water splitting, thus achieving a STH conversion efficiency value of about 3%. To the best of our knowledge, such value is the highest collected for unbiased PEC devices employing oxide composite materials for water splitting.

Niu et al. [49] synthesized a novel $Cu_2O/Ga_2O_3/TiO_2/RuO_x$ photocathode for water splitting able to achieve a maximum value of thermodynamically based energy conversion efficiency of about 1.9% at around +0.45 V versus RHE. The solar energy conversion efficiency was calculated using Eq. (2), where *J* is the photocurrent under AM 1.5 G irradiation, V_{RHE} is the applied potential versus RHE, $V(H^+/H_2)$ is the Nernst potential for hydrogen evolution (0 V vs RHE), and *P* is the incident solar irradiance (100 mW/cm^2 for AM 1.5 G).

$$\text{Energy conversion efficiency} = \frac{|J| \times \left[V_{RHE} - V\left(\frac{H^+}{H_2}\right)\right]}{P} \times 100\% \quad (2)$$

Such efficiency value, as expressed by Eq. (2), was the best found in the literature survey if compared with other Cu_2O/TiO_2 based photocathode structures under the same illumination conditions (i.e. AM 1.5 G), such as $FTO/Au/Cu_2O/AZO/TiO_2/Pt$ exhibiting an efficiency of 1.35% at 0.45 V [122–126].

As reported in Table 1, a number of further studies [18,65,69,72,77,80,89,127] expressed the maximum photoefficiency for hydrogen evolution in photoelectrochemical cells as photocurrent density (mA/cm^2) at different applied voltage values (i.e., 0.0 V versus reversible hydrogen electrode [65,80]). Such efficiency values are difficult to compare due to different illumination conditions, as in many cases the use of proper UV cut-off filters limiting light irradiation to the visible light spectral range ($\lambda > 400$ nm) is not considered.

Photocatalytic reactors

When evaluating photocatalytic hydrogen evolution activity over Cu_2O/TiO_2 composite materials, most of the researchers in the literature survey only reported indications on H_2 generation rate, in some cases per unit mass of catalyst, and compare such rate with the one recorded over basic catalyst (e.g., bare TiO_2) [3,60,65,66,68,79,84–86,92,105,110,118,120,128,129]. Due to such inconsistency between photoefficiency expressions and, once again, unequal light irradiation conditions, Cu_2O/TiO_2 photocatalyst performances for hydrogen generation turn out to be hard to compare, as shown in Table 1. To the best of our knowledge, amongst the highest values H_2 generation rate per unit mass of catalyst recorded under solar light irradiation only, Praveen Kumar et al. [88] obtained a value of 79.8 mmol/h g over a $Cu_2O/Cu(0)/TiO_2$ catalyst employed for the photoreforming of ethylene glycol under natural sunlight, with an average light intensity of 1.15 10^5 lx.

As listed in Table 1, column VIII [59,67,69,77], some authors also reported the values of Apparent Quantum Efficiency (AQE), as expressed by equation (3), where r_{H_2} (mol/time) the rate of hydrogen generation.

$$AQE = \frac{2 \times r_{H_2}}{\text{moles of incident photons/time}} \times 100 \quad (3)$$

Zhen et al. [69] recorded an AQE value for H_2 evolution of 45.7% over EY-sensitized $Cu/Cu_2O/Cu/TiO_2$ photocatalyst at 520 nm. Such ternary composite, prepared via an *in situ* photoreduction procedure, was tested for the photoreforming of TEOA in the presence of a 420 nm cut-off filter or various band-pass filters.

In general, however, with the aim of accomplishing a consistent comparison among different literature data, values of effective irradiation power should be specified, whereas only nominal power and lamp type were mostly reported in the experimental sections.

Conclusions

Cu_2O-based materials are used for a number of applications, such as sensing, desulfurization, disinfection, organic synthesis, photodegradation, photovoltaics, and photocatalysis. During last years, an intense scientific activity has been recorded in the field of hydrogen generation through photosplitting and organic photoreforming by combining Cu_2O and TiO_2.

Cu_2O is a p-type semiconductor exhibiting a narrow band gap (i.e. 2.2 eV), whereas TiO_2 is an extensively investigated n-type semiconductor. Their combination result in a p-n heterojunction, which (i) absorbs light radiation within the solar wavelength range and (ii) lowers the likelihood of photogenerated charge carrier recombination, thus improving the photocatalytic efficiency.

Clear guidance on the main techniques commonly adopted to characterize Cu_2O/TiO_2 composite materials have been herein described. In particular, details on characterization techniques aimed at (i) defining copper oxidation state (i.e. XRD, XPS, HR-TEM) and (ii) assessing the ability of Cu_2O/TiO_2 composites to absorb visible light irradiation and promote charge carrier separation (i.e. DRUV and PL) have been reported. As conflicting information on peaks in Raman spectra capable of uniquely identifying different copper oxidation states was found in the literature review, unambiguous data on Cu_2O and CuO species recording a general consensus by different Authors were thus selected.

Preparation method (e.g. chemical reduction, impregnation/calcination, electrochemical deposition, etc.), effect of pH and sacrificial organic species on HER, and chemical stability of Cu_2O/TiO_2 composites have been critically reviewed. Chemical reduction in the presence of titanium oxide via selected reducing agents (i.e. glucose, hydroxylamine, hydrazine, etc) turned out to be one the most commonly employed

preparation methods among the examples found during the literature survey. At the same time, samples prepared according to such method were capable to guarantee the highest increase in photoefficiency for HER with respect to bare TiO_2. The increase in pH until moderately alkaline values results in enhanced hydrogen production, due to high photocatalyst stability and absence of cupric ion release in the aqueous medium.

As regards the reaction mechanism, due to its capability to absorb visible light irradiation, cuprous oxide is broadly considered to act as energy antenna capable of transferring photogenerated electrons to TiO_2 and subsequently to proton ions which are reduced to hydrogen gas. Moreover, several authors report that the presence of selected co-catalysts, such as Cu (0), WS_2, Pt, Bi_2O_3, and Ga_2O_3 helps enhance photogenerated charge carrier separation, thus reducing their likelihood of recombination and promoting hydrogen evolution.

On the other hand, poor information on the efficiency for hydrogen generation of such materials under visible light irradiation has been recorded. The most relevant efficiency values collected over Cu_2O/TiO_2 photocatalysts, expressed through different indicators depending on the experimental setup adopted, have been reported. As regards photoelectrochemical cells, it should be mentioned that a STH conversion efficiency value of about 3% have been obtained over a $Cu/Cu_2O/Ga_2O_3/TiO_2$/NiMo photocathode for unassisted solar water splitting. As concerns photocatalytic reactors, an AQE value for H_2 evolution of 45.7% has been collected over EY-sensitized $Cu/Cu_2O/Cu/TiO_2$ photocatalyst at 520 nm. Overall, this is one of the major weakness affecting literature on hydrogen generation through photocatalytic processes.

Finally, the present literature review aims at clarifying some controversial indications found in the literature survey on the preparation, characterization, and use of Cu_2O/TiO_2 composites for HER), thus establishing a sound basis on which developing new efficient and cheap photocatalysts for hydrogen generation through solar photocatalytic processes.

Declaration of competing interest

The authors declare that they have no known competing financial interests or personal relationships that could have appeared to influence the work reported in this paper.

REFERENCES

[1] Osterloh FE, Parkinson BA. Recent developments in solar water-splitting photocatalysis. MRS Bull 2011;36:17–22. https://doi.org/10.1557/mrs.2010.5.

[2] Liu R, Zheng Z, Spurgeon J, Yang X. Enhanced photoelectrochemical water-splitting performance of semiconductors by surface passivation layers. Energy Environ Sci 2014;7:2504–17. https://doi.org/10.1039/c4ee00450g.

[3] Praveen Kumar D, Lakshmana Reddy N, Mamatha Kumari M, Srinivas B, Durga Kumari V, Sreedhar B, et al. Cu2O-sensitized TiO2 nanorods with nanocavities for highly efficient photocatalytic hydrogen production under solar irradiation. Sol Energy Mater Sol Cell 2015;136:157–66. https://doi.org/10.1016/j.solmat.2015.01.009.

[4] Zhang C, Fan W, Bai H, Yu X, Chen C, Zhang R, et al. Sandwich-Nanostructured NiO-ZnO Nanowires@α-Fe2O3 film photoanode with a synergistic effect and p-n junction for efficient photoelectrochemical water splitting. ChemElectroChem 2014;1:2089–97. https://doi.org/10.1002/celc.201402156.

[5] Jafary T, Wan Daud WR, Ghasemi M, Abu Bakar MH, Sedighi M, Kim BH, et al. Clean hydrogen production in a full biological microbial electrolysis cell. Int J Hydrogen Energy 2019;44:30524–31. https://doi.org/10.1016/j.ijhydene.2018.01.010.

[6] Keshavarzzadeh AH, Ahmadi P, Safaei MR. Assessment and optimization of an integrated energy system with electrolysis and fuel cells for electricity, cooling and hydrogen production using various optimization techniques. Int J Hydrogen Energy 2019;44:21379–96. https://doi.org/10.1016/j.ijhydene.2019.06.127.

[7] Zhang G, Zhou Y, Yang F. Hydrogen production from microbial fuel cells-ammonia electrolysis cell coupled system fed with landfill leachate using Mo2C/N-doped graphene nanocomposite as HER catalyst. Electrochim Acta 2019;299:672–81. https://doi.org/10.1016/j.electacta.2019.01.055.

[8] Jing D, Guo L, Zhao L, Zhang X, Liu H, Li M, et al. Efficient solar hydrogen production by photocatalytic water splitting: from fundamental study to pilot demonstration. Int J Hydrogen Energy 2010;35:7087–97. https://doi.org/10.1016/j.ijhydene.2010.01.030.

[9] Tong H, Ouyang S, Bi Y, Umezawa N, Oshikiri M, Ye J. Nano-photocatalytic materials: possibilities and challenges. Adv Mater 2012;24:229–51. https://doi.org/10.1002/adma.201102752.

[10] Fajrina N, Tahir M. A critical review in strategies to improve photocatalytic water splitting towards hydrogen production. Int J Hydrogen Energy 2019;44:540–77. https://doi.org/10.1016/j.ijhydene.2018.10.200.

[11] Kim CS, Moon BK, Park JH, Choi BC, Seo HJ. Solvothermal synthesis of nanocrystalline TiO2 in toluene with surfactant. J Cryst Growth 2003;257:309–15. https://doi.org/10.1016/S0022-0248(03)01468-4.

[12] Thakur S, Kumar J. Structural and optical properties of copper doped ZnO nanoparticles and thin films ZnO as dilute magnetic semiconductor view project dilute magnetic semiconductor view project. 2014.

[13] Kolb MJ, Wermink J, Calle-Vallejo F, Juurlink LBF, Koper MTM. Initial stages of water solvation of stepped platinum surfaces. Phys Chem Chem Phys 2016;18:3416–22. https://doi.org/10.1039/c5cp04468e.

[14] Finegold L, Cude JL. Biological sciences: one and two-dimensional structure of alpha-helix and beta-sheet forms of poly(L-Alanine) shown by specific heat measurements at low temperatures (1.5-20 K). Nature 1972;238:38–40. https://doi.org/10.1038/238038a0.

[15] Ong WL, Gao M, Ho GW. Hybrid organic PVDF-inorganic M-rGO-TiO2 (M = Ag, Pt) nanocomposites for multifunctional volatile organic compound sensing and photocatalytic degradation-H2 production. Nanoscale 2013;5:11283–90. https://doi.org/10.1039/c3nr03276k.

[16] Wong TJ, Lim FJ, Gao M, Lee GH, Ho GW. Photocatalytic H2 production of composite one-dimensional TiO2 nanostructures of different morphological structures and crystal phases with graphene. Catal Sci Technol 2013;3:1086–93. https://doi.org/10.1039/c2cy20740k.

[17] Wang J, Ng YH, Lim YF, Ho GW. Vegetable-extracted carbon dots and their nanocomposites for enhanced photocatalytic

H2 production. RSC Adv 2014;4:44117–23. https://doi.org/10.1039/c4ra07290a.
[18] Yuan W, Yuan J, Xie J, Li CM. Polymer-mediated self-assembly of TiO2@Cu2O core-shell nanowire array for highly efficient photoelectrochemical water oxidation. ACS Appl Mater Interfaces 2016;8:6082–92. https://doi.org/10.1021/acsami.6b00030.
[19] Kumaravel V, Mathew S, Bartlett J, Pillai SC. Photocatalytic hydrogen production using metal doped TiO2: a review of recent advances. Appl Catal B Environ 2019;244:1021–64. https://doi.org/10.1016/j.apcatb.2018.11.080.
[20] Samsudin EM, Abd Hamid SB. Effect of band gap engineering in anionic-doped TiO2 photocatalyst. Appl Surf Sci 2017;391:326–36. https://doi.org/10.1016/j.apsusc.2016.07.007.
[21] Dholam R, Patel N, Adami M, Miotello A. Hydrogen production by photocatalytic water-splitting using Cr- or Fe-doped TiO2 composite thin films photocatalyst. Int J Hydrogen Energy 2009;34:5337–46. https://doi.org/10.1016/j.ijhydene.2009.05.011.
[22] Yang Y, Li XJ, Chen JT, Wang LY. Effect of doping mode on the photocatalytic activities of Mo/TiO2. J Photochem Photobiol Chem 2004;163:517–22. https://doi.org/10.1016/j.jphotochem.2004.02.008.
[23] Jia L, Wu C, Han S, Yao N, Li Y, Li Z, et al. Theoretical study on the electronic and optical properties of (N, Fe)-codoped anatase TiO2 photocatalyst. J Alloys Compd 2011;509:6067–71. https://doi.org/10.1016/j.jallcom.2011.03.012.
[24] Xu S, Ng J, Zhang X, Bai H, Sun DD. Fabrication and comparison of highly efficient Cu incorporated TiO2 photocatalyst for hydrogen generation from water. Int J Hydrogen Energy 2010;35:5254–61. https://doi.org/10.1016/j.ijhydene.2010.02.129.
[25] Gogoi D, Namdeo A, Golder AK, Peela NR. Ag-doped TiO2 photocatalysts with effective charge transfer for highly efficient hydrogen production through water splitting. Int J Hydrogen Energy 2020;45:2729–44. https://doi.org/10.1016/j.ijhydene.2019.11.127.
[26] Ni M, Leung MKH, Leung DYC, Sumathy K. A review and recent developments in photocatalytic water-splitting using TiO2 for hydrogen production. Renew Sustain Energy Rev 2007;11:401–25. https://doi.org/10.1016/j.rser.2005.01.009.
[27] Choi HJ, Kang M, Graves JE, Bowker MEA, Summer A, Greenwood A, et al. Hydrogen production from methanol/water decomposition in a liquid photosystem using the anatase structure of Cu loaded TiO2. Bull Kor Chem Soc 2007;35:3841–8. https://doi.org/10.5012/bkcs.2014.35.1.309.
[28] Clarizia L, Spasiano D, Di Somma I, Marotta R, Andreozzi R, Dionysiou DD. Copper modified-TiO2 catalysts for hydrogen generation through photoreforming of organics. A short review. Int J Hydrogen Energy 2014;39:16812–31. https://doi.org/10.1016/j.ijhydene.2014.08.037.
[29] Byrne C, Moran L, Hermosilla D, Merayo N, Blanco Á, Rhatigan S, et al. Effect of Cu doping on the anatase-to-rutile phase transition in TiO2 photocatalysts: theory and experiments. Appl Catal B Environ 2019;246:266–76. https://doi.org/10.1016/j.apcatb.2019.01.058.
[30] Mathew S, Ganguly P, Rhatigan S, Kumaravel V, Byrne C, Hinder SJ, et al. Cu-Doped TiO2: visible light assisted photocatalytic antimicrobial activity. Appl Sci 2018;vol. 8. https://doi.org/10.3390/app8112067.
[31] Cao S, Chen H, Han T, Zhao C, Peng L. Rose-like Cu2O nanoflowers via hydrothermal synthesis and their gas sensing properties. Mater Lett 2016;180:135–9. https://doi.org/10.1016/j.matlet.2016.05.105.
[32] Nagase K, Zheng Y, Kodama Y, Kakuta J. Dynamic study of the oxidation state of copper in the course of carbon monoxide oxidation over powdered CuO and Cu2O. J Catal 1999;187:123–30. https://doi.org/10.1006/jcat.1999.2611.
[33] Bessekhouad Y, Robert D, Weber JV. Photocatalytic activity of Cu2O/TiO2, Bi2O3/TiO2 and ZnMn2O4/TiO2 heterojunctions. Catal Today 2005;101:315–21. https://doi.org/10.1016/j.cattod.2005.03.038.
[34] Zhang W, Shi L, Tang K, Dou S, Khan R, Ahmad R, et al. Controllable synthesis of Cu2O microcrystals via a complexant-assisted synthetic route. Sensor Actuator B Chem 2010;203:471–6. https://doi.org/10.1016/j.snb.2014.06.128.
[35] Nakano Y, Saeki S, Morikawa T. Optical bandgap widening of p -type Cu2O films by nitrogen doping. Appl Phys Lett 2009;94:1–4. https://doi.org/10.1063/1.3072804.
[36] Kakuta S, Abe T. Structural characterization of Cu2O after the evolution of H2 under visible light irradiation. Electrochem Solid State Lett 2009;12:2–5. https://doi.org/10.1149/1.3054330.
[37] Susman MD, Feldman Y, Vaskevich A, Rubinstein I. Chemical deposition of Cu2O nanocrystals with precise morphology control. ACS Nano 2014;8:162–74. https://doi.org/10.1021/nn405891g.
[38] Clarizia L, Vitiello G, Pallotti DK, Silvestri B, Nadagouda M, Lettieri S, et al. Effect of surface properties of copper-modified commercial titanium dioxide photocatalysts on hydrogen production through photoreforming of alcohols. Int J Hydrogen Energy 2017;42:28349–62. https://doi.org/10.1016/j.ijhydene.2017.09.093.
[39] Khan R, Ahmad R, Rai P, Jang LW, Yun JH, Yu YT, et al. Glucose-assisted synthesis of Cu2O shuriken-like nanostructures and their application as nonenzymatic glucose biosensors. Sensor Actuator B Chem 2014;203:471–6. https://doi.org/10.1016/j.snb.2014.06.128.
[40] Wang S, Wang W, Yue L, Cui S, Wang H, Wang C, et al. Hierarchical Cu2O nanowires covered by silver nanoparticles-doped carbon layer supported on Cu foam for rapid and efficient water disinfection with lower voltage. Chem Eng J 2020;382:122855. https://doi.org/10.1016/j.cej.2019.122855.
[41] Manisha H, Priya Swetha PD, Shim YB, Prasad KS. Microwave assisted synthesis of hybrid Cu2O microcubes for photocatalysis and electrocatalysis. Mater Today: Proceedings 2018;5:16390–3. https://doi.org/10.1016/j.matpr.2018.05.135.
[42] Rubino A, Schiavi PG, Altimari P, Latini A, Pagnanelli F. Ti/TiO2/Cu2O based electrodes as photocatalysts in PEC cells. Chem Eng Trans 2019;73:73–8. https://doi.org/10.3303/CET1973013.
[43] Zimbovskii DS, Baranov AN. Synthesis of Cu2O-based heterostructures and their photocatalytic properties for water splitting. Inorg Mater 2020;56:366–73. https://doi.org/10.1134/S0020168520040159.
[44] Kou J, Lu C, Sun W, Zhang L, Xu Z. Facile fabrication of cuprous oxide-based adsorbents for deep desulfurization. ACS Sustainable Chem Eng 2015;3:3053–61. https://doi.org/10.1021/acssuschemeng.5b01051.
[45] Singh G, Kumar M, Sharma K, Bhalla V. A supramolecular ensemble of a PBI derivative and Cu2O NPs: potential photocatalysts for the Suzuki and Suzuki type coupling reactions. Green Chem 2016;18:3278–85. https://doi.org/10.1039/c5gc03012a.
[46] Li P, Lv W, Ai S. Green and gentle synthesis of Cu2O nanoparticles using lignin as reducing and capping reagent with antibacterial properties. J Exp Nanosci 2016;11:18–27. https://doi.org/10.1080/17458080.2015.1015462.
[47] Wang J, Ng Y Hwee, Lim Y, Ho GW. Vegetable-extracted carbon dots and their nanocomposites for enhanced

photocatalytic H2 production. RSC Adv 2014;4:44117–23. https://doi.org/10.1017/CBO9781107415324.004.
[48] Jing M, Cui P, Liu K. Research status and development of Cu2O Thin Film film solar cells. Mater Sci Forum 2017;893:151–5. https://doi.org/10.4028/www.scientific.net/MSF.893.151. MSF.
[49] Niu W, Moehl T, Cui W, Wick-Joliat R, Zhu L, Tilley SD. Extended light harvesting with dual Cu2O-based photocathodes for high efficiency water splitting. Adv Energy Mater 2018;8:1–8. https://doi.org/10.1002/aenm.201702323.
[50] Yang Z, Ma C, Wang W, Zhang M, Hao X, Chen S. Fabrication of Cu2O-Ag nanocomposites with enhanced durability and bactericidal activity. J Colloid Interface Sci 2019;557:156–67. https://doi.org/10.1016/j.jcis.2019.09.015.
[51] Liu B, Wu Y, Zhang J, Han X, Shi H. Visible-light-driven g-C3N4/Cu2O heterostructures with efficient photocatalytic activities for tetracycline degradation and microbial inactivation. J Photochem Photobiol Chem 2019;378:1–8. https://doi.org/10.1016/j.jphotochem.2019.04.007.
[52] Luévano-Hipólito E, Torres-Martínez LM, Sánchez-Martínez D, Alfaro Cruz MR. Cu2O precipitation-assisted with ultrasound and microwave radiation for photocatalytic hydrogen production. Int J Hydrogen Energy 2017;42:12997–3010. https://doi.org/10.1016/j.ijhydene.2017.03.192.
[53] Minami T, Nishi Y, Miyata T. Cu2O-based solar cells using oxide semiconductors. J Semiconduct 2016;37. https://doi.org/10.1088/1674-4926/37/1/014002.
[54] Cho YS, Huh YD. Microwave assisted synthesis of Cu2O crystals with morphological evolution from octapod to octahedron. Bull Kor Chem Soc 2014;35:309–12. https://doi.org/10.5012/bkcs.2014.35.1.309.
[55] Oros-Ruiz S, Zanella R, Collins SE, Hernández-Gordillo A, Gómez R. Photocatalytic hydrogen production by Au-MxOy (MAg, Cu, Ni) catalysts supported on TiO2. Catal Commun 2014. https://doi.org/10.1016/j.catcom.2013.12.033.
[56] Fu J, Cao S, Yu J. Dual Z-scheme charge transfer in TiO2–Ag–Cu2O composite for enhanced photocatalytic hydrogen generation. J Materiomics 2015. https://doi.org/10.1016/j.jmat.2015.02.002.
[57] Sinatra L, Lagrow AP, Peng W, Kirmani AR, Amassian A, Idriss H, et al. A Au/Cu2O-TiO2 system for photo-catalytic hydrogen production. A pn-junction effect or a simple case of in situ reduction? J Catal 2015. https://doi.org/10.1016/j.jcat.2014.11.012.
[58] Lalitha K, Sadanandam G, Kumari VD, Subrahmanyam M, Sreedhar B, Hebalkar NY. Highly stabilized and finely dispersed Cu2O/TiO2: a promising visible sensitive photocatalyst for continuous production of hydrogen from glycerol:water mixtures. J Phys Chem C 2010;114:22181–9. https://doi.org/10.1021/jp107405u.
[59] Li L, Xu L, Shi W, Guan J. Facile preparation and size-dependent photocatalytic activity of Cu 2O nanocrystals modified titania for hydrogen evolution. Int J Hydrogen Energy 2013;38:816–22. https://doi.org/10.1016/j.ijhydene.2012.10.064.
[60] Xi Z, Li C, Zhang L, Xing M, Zhang J. Synergistic effect of Cu2O/TiO2 heterostructure nanoparticle and its high H2 evolution activity. Int J Hydrogen Energy 2014;39:6345–53. https://doi.org/10.1016/j.ijhydene.2014.01.209.
[61] Xu H, Ouyang S, Liu L, Wang D, Kako T, Ye J. Porous-structured Cu2O/TiO2 nanojunction material toward efficient CO2 photoreduction. Nanotechnology 2014;25. https://doi.org/10.1088/0957-4484/25/16/165402.
[62] Wang M, Sun L, Lin Z, Cai J, Xie K, Lin C. P-n Heterojunction photoelectrodes composed of Cu2O-loaded TiO2 nanotube arrays with enhanced photoelectrochemical and photoelectrocatalytic activities. Energy Environ Sci 2013;6:1211–20. https://doi.org/10.1039/c3ee24162a.
[63] Moniz SJA, Shevlin SA, Martin DJ, Guo ZX, Tang J. Visible-light driven heterojunction photocatalysts for water splitting-a critical review. Energy Environ Sci 2015;8:731–59. https://doi.org/10.1039/c4ee03271c.
[64] Zheng Xing, Xu Zong, Jian Pan LW. On the engineering part of solar hydrogen production from water splitting: photoreactor design. Chem Eng Sci 2013:125–46. https://doi.org/10.1016/j.ces.2013.08.039.
[65] Long B, Yang H, Li M, Balogun MS, Mai W, Ouyang G, et al. Interface charges redistribution enhanced monolithic etched copper foam-based Cu2O layer/TiO2 nanodots heterojunction with high hydrogen evolution electrocatalytic activity. Appl Catal B Environ 2019;243:365–72. https://doi.org/10.1016/j.apcatb.2018.10.039.
[66] Segovia-Guzmán MO, Román-Aguirre M, Verde-Gomez JY, Collins-Martínez VH, Zaragoza-Galán G, Ramos-Sánchez VH. Green Cu2O/TiO2 heterojunction for glycerol photoreforming. Catal Today 2018. https://doi.org/10.1016/j.cattod.2018.05.031.
[67] Tamiolakis I, Papadas IT, Spyridopoulos KC, Armatas GS. Mesoporous assembled structures of Cu2O and TiO2 nanoparticles for highly efficient photocatalytic hydrogen generation from water. RSC Adv 2016;6:54848–55. https://doi.org/10.1039/c6ra08546f.
[68] Cheng WY, Yu TH, Chao KJ, Lu SY. Cu2O-decorated mesoporous TiO2 beads as a highly efficient photocatalyst for hydrogen production. ChemCatChem 2014;6:293–300. https://doi.org/10.1002/cctc.201300681.
[69] Zhen W, Jiao W, Wu Y, Jing H, Lu G. The role of a metallic copper interlayer during visible photocatalytic hydrogen generation over a Cu/Cu2O/Cu/TiO2 catalyst. Catal Sci Technol 2017;7:5028–37. https://doi.org/10.1039/c7cy01432e.
[70] Zhu W, Chong B, Qin K, Guan L, Hou X, Chen GZ. Cuprous oxide/titanium dioxide nanotube-array with coaxial heterogeneous structure synthesized by multiple-cycle chemical adsorption plus reduction method. RSC Adv 2016;6:59160–8. https://doi.org/10.1039/c6ra06893f.
[71] Le L, Wu Y, Zhou Z, Wang H, Xiong R, Shi J. Cu2O clusters decorated on flower-like TiO2 nanorod array film for enhanced hydrogen production under solar light irradiation. J Photochem Photobiol Chem 2018;351:78–86. https://doi.org/10.1016/j.jphotochem.2017.08.073.
[72] Li X, Liu B, Chen Y, Fan X, Li Y, Zhang F, et al. Decoration of Cu2O photocathode with protective TiO2 and active WS2 layers for enhanced photoelectrochemical hydrogen evolution. Nanotechnology 2018;29. https://doi.org/10.1088/1361-6528/aae569.
[73] Tsui LK, Zangari G. The influence of morphology of electrodeposited Cu2O and Fe2O3 on the conversion efficiency of TiO2 nanotube photoelectrochemical solar cells. Electrochim Acta 2013;100:220–5. https://doi.org/10.1016/j.electacta.2012.07.058.
[74] Li Y, Wang B, Liu S, Duan X, Hu Z. Synthesis and characterization of Cu2O/TiO2 photocatalysts for H2 evolution from aqueous solution with different scavengers. Appl Surf Sci 2015;324:736–44. https://doi.org/10.1016/j.apsusc.2014.11.027.
[75] Wang Y, Cao S, Huan Y, Nie T, Ji Z, Bai Z, et al. The effect of composite catalyst on Cu2O/TiO2 heterojunction photocathodes for efficient water splitting. Appl Surf Sci 2020;526. https://doi.org/10.1016/j.apsusc.2020.146700.
[76] Pan L, Kim JH, Mayer MT, Son MK, Ummadisingu A, Lee JS, et al. Boosting the performance of Cu2O photocathodes for

unassisted solar water splitting devices. Nat Catal 2018;1:412–20. https://doi.org/10.1038/s41929-018-0077-6.
[77] Das C, Ananthoju B, Dhara AK, Aslam M, Sarkar SK, Balasubramaniam KR. Electron-selective TiO2/CVD-graphene layers for photocorrosion inhibition in Cu2O photocathodes. Adv Mater Interface 2017;4:1–10. https://doi.org/10.1002/admi.201700271.
[78] Wang X, Dong H, Hu Z, Qi Z, Li L. Fabrication of a Cu2O/Au/TiO2composite film for efficient photocatalytic hydrogen production from aqueous solution of methanol and glucose. Mater Sci Eng B: Solid state Mater Adv Technol 2017;219:10–9. https://doi.org/10.1016/j.mseb.2017.02.011.
[79] Hu Z, Wang X, Dong H, Li S, Li X, Li L. Efficient photocatalytic degradation of tetrabromodiphenyl ethers and simultaneous hydrogen production by TiO2-Cu2O composite films in N2atmosphere: influencing factors, kinetics and mechanism. J Hazard Mater 2017;340:1–15. https://doi.org/10.1016/j.jhazmat.2017.07.009.
[80] Choi J, Song JT, Jang HS, Choi MJ, Sim DM, Yim S, et al. Interfacial band-edge engineered TiO2 protection layer on Cu2O photocathodes for efficient water reduction reaction. Electron Mater Lett 2017;13:57–65. https://doi.org/10.1007/s13391-017-6316-1.
[81] Chang KL, Sun Q, Peng YP, Lai SW, Sung M, Huang CY, et al. Cu2O loaded titanate nanotube arrays for simultaneously photoelectrochemical ibuprofen oxidation and hydrogen generation. Chemosphere 2016;150:605–14. https://doi.org/10.1016/j.chemosphere.2016.02.016.
[82] Nishikawa M, Fukuda M, Nakabayashi Y, Saito N, Ogawa N, Nakajima T, et al. A method to give chemically stabilities of photoelectrodes for water splitting: compositing of a highly crystalized TiO 2 layer on a chemically unstable Cu 2 O photocathode using laser-induced crystallization process. Appl Surf Sci 2016;363:173–80. https://doi.org/10.1016/j.apsusc.2015.12.002.
[83] Zhang S, Peng B, Yang S, Fang Y, Peng F. The influence of the electrodeposition potential on the morphology of Cu2O/TiO2 nanotube arrays and their visible-light-driven photocatalytic activity for hydrogen evolution. Int J Hydrogen Energy 2013;38:13866–71. https://doi.org/10.1016/j.ijhydene.2013.08.081.
[84] Trang TNQ, Tu LTN, Man TV, Mathesh M, Nam ND, Thu VTH. A high-efficiency photoelectrochemistry of Cu2O/TiO2 nanotubes based composite for hydrogen evolution under sunlight. Compos B Eng 2019;174. https://doi.org/10.1016/j.compositesb.2019.106969.
[85] Liu Y, Ye Z, Li D, Wang M, Zhang Y, Huang W. Tuning CuOx -TiO2 interaction and photocatalytic hydrogen production of CuOx/TiO2 photocatalysts via TiO2 morphology engineering. Appl Surf Sci 2019;473:500–10. https://doi.org/10.1016/j.apsusc.2018.12.177.
[86] Bharad PA, Nikam AV, Thomas F, Gopinath CS. CuOx-TiO2 composites: electronically integrated nanocomposites for solar hydrogen generation. ChemistrySelect 2018;3:12022–30. https://doi.org/10.1002/slct.201802047.
[87] Liu Y, Wang Z, Huang W. Influences of TiO2 phase structures on the structures and photocatalytic hydrogen production of CuOx/TiO2 photocatalysts. Appl Surf Sci 2016;389:760–7. https://doi.org/10.1016/j.apsusc.2016.07.173.
[88] Praveen Kumar D, Lakshmana Reddy N, Srinivas B, Durgakumari V, Roddatis V, Bondarchuk O, et al. Stable and active CuxO/TiO2 nanostructured catalyst for proficient hydrogen production under solar light irradiation. Sol Energy Mater Sol Cell 2016;146:63–71. https://doi.org/10.1016/j.solmat.2015.11.030.
[89] Dubey PK, Kumar R, Tiwari RS, Srivastava ON, Pandey AC, Singh P. Surface modification of aligned TiO2 nanotubes by Cu2O nanoparticles and their enhanced photo electrochemical properties and hydrogen generation application. Int J Hydrogen Energy 2018;43:6867–78. https://doi.org/10.1016/j.ijhydene.2018.02.127.
[90] Clarizia L, Vitiello G, Luciani G, Di Somma I, Andreozzi R, Marotta R. In situ photodeposited nanoCu on TiO2 as a catalyst for hydrogen production under UV/visible radiation. Appl Catal Gen 2016;518:142–9. https://doi.org/10.1016/j.apcata.2015.07.044.
[91] Ingunta R, Piazza S, Sunseri C. Novel procedure for the template synthesis of metal nanostructures. Electrochem Commun 2008;506–9.
[92] Jung M, Hart JN, Scott J, Ng YH, Jiang Y, Amal R. Exploring Cu oxidation state on TiO2 and its transformation during photocatalytic hydrogen evolution. Appl Catal Gen 2016;521:190–201. https://doi.org/10.1016/j.apcata.2015.11.013.
[93] Hu Q, Huang J, Li G, Chen J, Zhang Z, Deng Z, et al. Effective water splitting using CuO x/TiO 2 composite films: role of Cu species and content in hydrogen generation. Appl Surf Sci 2016;369:201–6. https://doi.org/10.1016/j.apsusc.2016.01.281.
[94] Kilo M, Schild C, Wokaun A, Baiker A. Surface oxidic phases of binary and ternary zirconia-supported metal catalysts investigated by Raman spectroscopy. J Chem Soc, Faraday Trans 1992;88:1453–7. https://doi.org/10.1039/FT9928801453.
[95] Niaura G. Surface-enhanced Raman spectroscopic observation of two kinds of adsorbed OH− ions at copper electrode. Electrochim Acta 2000;45:3507–19.
[96] Compaan A, Cummins HZ. Raman scattering, luminescence, and exciton-phonon coupling in Cu2O. Phys Rev B 1972;6:4753.
[97] Xu JF, Ji W, Shen ZX, Tang SH, Ye XR, Jia DZ, Xin XQ. Preparation and characterization of CuO nanocrystals. J Solid State Chem 1999;147:516–9. https://doi.org/10.1006/jssc.1999.8409.
[98] Chan Ho Yeung H, Takoudis Christos G, Weaver MJ. Electrochemical control of gas-phase oxidation and reduction of copper as probed by surface-enhanced Raman spectroscopy. Electrochem Solid State Lett 1999;2:189.
[99] Muller RH. An in situ Roman spectroscopy study of the anodic oxidation of copper in alkaline media. J Electrochem Soc 1992;139:426–34. https://doi.org/10.1149/1.2069234.
[100] Hamilton JC, Farmer JC, Anderson RJ. In situ Raman spectroscopy of anodic films formed on copper and silver in sodium hydroxide solution. J Electrochem Soc 1986;133:739–45. https://doi.org/10.1149/1.2108666.
[101] Vitiello G, Clarizia L, Abdelraheem W, Esposito S, Bonelli B, Ditaranto N, et al. Near UV-irradiation of CuOx-impregnated TiO2 providing active species for H2 production through methanol photoreforming. ChemCatChem 2019;11:4314–26. https://doi.org/10.1002/cctc.201900818.
[102] Li Z, Liu J, Wang D, Gao Y, Shen J. Cu2O/Cu/TiO2 nanotube Ohmic heterojunction arrays with enhanced photocatalytic hydrogen production activity. Int J Hydrogen Energy 2012. https://doi.org/10.1016/j.ijhydene.2012.01.075.
[103] Oku T, Motoyoshi R, Fujimoto K, Akiyama T, Jeyadevan B, Cuya J. Structures and photovoltaic properties of copper oxides/fullerene solar cells. J Phys Chem Solid 2011;72:1206–11.
[104] Zhou T, Zang Z, Wei J, Zheng J, Hao J, Ling F. Efficient charge carrier separation and excellent visible light photoresponse

in Cu2O nanowires. Nano Energy 2018;50:118–25. https://doi.org/10.1016/j.nanoen.2018.05.028.
[105] Police AKR, Vattikuti SVP, Mandari KK, Chennaiahgari M, Phanikrishna PS, Valluri DK, et al. Bismuth oxide cocatalyst and copper oxide sensitizer in Cu2O/TiO2/Bi2O3 ternary photocatalyst for efficient hydrogen production under solar light irradiation. Ceram Int 2018;44:11783–91. https://doi.org/10.1016/j.ceramint.2018.03.262.
[106] Yan L, Yang F, Tao CY, Luo X, Zhang L. Highly efficient and stable Cu2O–TiO2 intermediate photocatalytic water splitting. Ceram Int 2020;46:9455–63. https://doi.org/10.1016/j.ceramint.2019.12.206.
[107] Yu J-G, Yu H-G, Cheng B, Zhao X-J, Yu JC, Ho W-K. The effect of calcination temperature on the surface microstructure and photocatalytic activity of TiO2 thin films prepared by liquid phase deposition. J Phys Chem B 2003;107:13871–9. https://doi.org/10.1021/jp036158y.
[108] Huang Lei, Peng Feng, Wang Hongjuan, Yu Hao, Li Z. Preparation and characterization of Cu2O/TiO2 nano–nano heterostructure photocatalysts. Catal Commun 2009;10:1839–43.
[109] Wang J, Chen Z, Zhai G, Men Y. Boosting photocatalytic activity of WO3 nanorods with tailored surface oxygen vacancies for selective alcohol oxidations. Appl Surf Sci 2018;462:760–71. https://doi.org/10.1016/j.apsusc.2018.08.181.
[110] Majeed I, Nadeem MA, Badshah A, Kanodarwala FK, Ali H, Khan MA, et al. Titania supported MOF-199 derived Cu-Cu2O nanoparticles: highly efficient non-noble metal photocatalysts for hydrogen production from alcohol-water mixtures. Catal Sci Technol 2017;7:677–86. https://doi.org/10.1039/c6cy02328b.
[111] Ahmad Rather R. A Cu+1/Cu0-TiO2 mesoporous nanocomposite exhibits improved H2 production from H2O under direct solar irradiation. J Catal 2017;346:1–9. https://doi.org/10.1016/j.jcat.2016.11.021.
[112] Ahmad H, Kamarudin SK, Minggu LJ, Kassim M. Hydrogen from photo-catalytic water splitting process: a review. Renew Sustain Energy Rev 2015;43:599–610. https://doi.org/10.1016/j.rser.2014.10.101.
[113] Han B, Hu YH. Highly efficient temperature-induced visible light photocatalytic hydrogen production from water. J Phys Chem C 2015;119:18927–34. https://doi.org/10.1021/acs.jpcc.5b04894.
[114] Zhang YH, Li YL, Jiu BB, Gong FL, Chen JL, Fang SM, et al. Highly enhanced photocatalytic H2 evolution of Cu2O microcube by coupling with TiO2 nanoparticles. Nanotechnology 2019;30. https://doi.org/10.1088/1361-6528/aafccb.
[115] Peng C, Xu W, Wei P, Liu MC, Guo L, Wu P, et al. Manipulating photocatalytic pathway and activity of ternary Cu2O/(001)TiO2@Ti3C2Tx catalysts for H2 evolution: effect of surface coverage. Int J Hydrogen Energy 2019;44:29975–85. https://doi.org/10.1016/j.ijhydene.2019.09.190.
[116] Wei T, Zhu YN, An X, Liu LM, Cao X, Liu H, et al. Defect modulation of Z-scheme TiO2/Cu2O photocatalysts for durable water splitting. ACS Catal 2019;9:8346–54. https://doi.org/10.1021/acscatal.9b01786.
[117] Li G, Huang J, Deng Z, Chen J, Huang Q, Liu Z, et al. Highly active photocatalyst of CuOx modified TiO2 arrays for hydrogen generation. Cryst Growth Des 2019;19:5784–90. https://doi.org/10.1021/acs.cgd.9b00797.
[118] Li G, Huang J, Chen J, Deng Z, Huang Q, Liu Z, et al. Highly active photocatalyst of Cu 2 O/TiO 2 octahedron for hydrogen generation. ACS Omega 2019;4:3392–7. https://doi.org/10.1021/acsomega.8b03404.
[119] Hu Q, Huang J, Li G, Jiang Y, Lan H, Guo W, et al. Origin of the improved photocatalytic activity of Cu incorporated TiO2 for hydrogen generation from water. Appl Surf Sci 2016;382:170–7. https://doi.org/10.1016/j.apsusc.2016.04.126.
[120] Kum JM, Park YJ, Kim HJ, Cho SO. Plasmon-enhanced photocatalytic hydrogen production over visible-light responsive Cu/TiO2. Nanotechnology 2015;26. https://doi.org/10.1088/0957-4484/26/12/125402.
[121] Dotan H, Mathews N, Hisatomi T, Grätzel M, Rothschild A. On the solar to hydrogen conversion efficiency of photoelectrodes for water splitting. J Phys Chem Lett 2014;5:3330–4. https://doi.org/10.1021/jz501716g.
[122] Paracchino Adriana, Mathews Nripan, Hisatomi Takashi, Stefik Morgan, Tilley S David, Grätzel M. Ultrathin films on copper(i) oxide water splitting photocathodes: a study on performance and stability. Energy Environ Sci 2012;5:8673–81.
[123] Azevedo J, Steier L, Dias P, Stefik M, Sousa CT, Araújo JP, Mendes A, Graetzel M, Tilley SD. On the stability enhancement of cuprous oxide water splitting photocathodes by low temperature steam annealing. Energy Environ Sci 2014;7:4044–52.
[124] Dai P, Li W, Xie J, He Y, Thorne J, McMahon G, et al. Forming buried junctions to enhance the photovoltage generated by cuprous oxide in aqueous solutions. Angew Chem Int Ed 2014;53:13493–7. https://doi.org/10.1002/anie.201408375.
[125] Li C, Hisatomi T, Watanabe O, Nakabayashi M. Positive onset potential and stability of Cu2O-based photocathodes in water splitting by atomic layer deposition of a Ga2O3 buffer layer. Energy Environ Sci 2015:1493–500. https://doi.org/10.1039/c5ee00250h.
[126] Luo J, Steier L, Son M-K, Schreier M, Mayer MT, Grätzel M. Cu2O nanowire photocathodes for efficient and durable solar water splitting. Nano Lett 2016;16:1848–57. https://doi.org/10.1021/acs.nanolett.5b04929.
[127] Yao L, Wang W, Wang L, Liang Y, Fu J, Shi H. Chemical bath deposition synthesis of TiO2/Cu2O core/shell nanowire arrays with enhanced photoelectrochemical water splitting for H2 evolution and photostability. Int J Hydrogen Energy 2018;43:15907–17. https://doi.org/10.1016/j.ijhydene.2018.06.127.
[128] Deng C, Hong R, Jing M, Shi J, Yan T, Tao C, et al. Photocatalytic performance of TiO2 thin film decorated with Cu2O nanoparticles by laser ablation. Opt Mater 2019;94:130–7. https://doi.org/10.1016/j.optmat.2019.05.030.
[129] Hinojosa-Reyes M, Camposeco-Solís R, Zanella R, Rodríguez González V. Hydrogen production by tailoring the brookite and Cu2O ratio of sol-gel Cu-TiO2 photocatalysts. Chemosphere 2017;184:992–1002. https://doi.org/10.1016/j.chemosphere.2017.06.066.
[130] Zhao K, Zhao S, Qi J, Yin H, Gao C, Khattak AM, et al. Cu2O clusters grown on TiO2 nanoplates as efficient photocatalysts for hydrogen generation. Inorg Chem Front 2016;3:488–93. https://doi.org/10.1039/C5QI00284B.
[131] Gao H, Zhang J, Wang R, Wang M. Highly efficient hydrogen production and formaldehyde degradation by Cu2O microcrystals. Appl Catal B Environ 2015;172–173:1–6. https://doi.org/10.1016/j.apcatb.2015.02.004.

[132] Sang L, Zhang J, Zhang Y, Zhao Y, Lin J. Preparation of Cu 2 O/TiO 2 nanotube arrays and their photoelectrochemical properties as hydrogen-evolving photoanode, vol. 9560. Proc. SPIE 9560, Solar Hydrogen and Nanotechnology X; 2015. p. 1–9.

[133] Devadoss A, Sudhagar P, Ravidhas C, Hishinuma R, Terashima C, Nakata K, et al. Simultaneous glucose sensing and biohydrogen evolution from direct photoelectrocatalytic glucose oxidation on robust Cu2O-TiO2 electrodes. Phys Chem Chem Phys 2014;16:21237–42. https://doi.org/10.1039/c4cp03262d.

[134] Zhu L, Junying Z, Chen Z, Liu K, Gao H. Effect of Cu2O morphology on photocatalytic hydrogen generation and chemical stability of TiO2/Cu2O composite. J Nanosci Nanotechnol 2013;13:5104–8. https://doi.org/10.1166/jnn.2013.7591.

[135] Luo L, Zhang T, Zhang X, Rongping Y, Yanjun L, Bing Z, et al. Enhanced hydrogen production from ethanol photoreforming by site-specific deposition of Au on Cu2O/TiO2 p-n junction. Catalysts 2020.